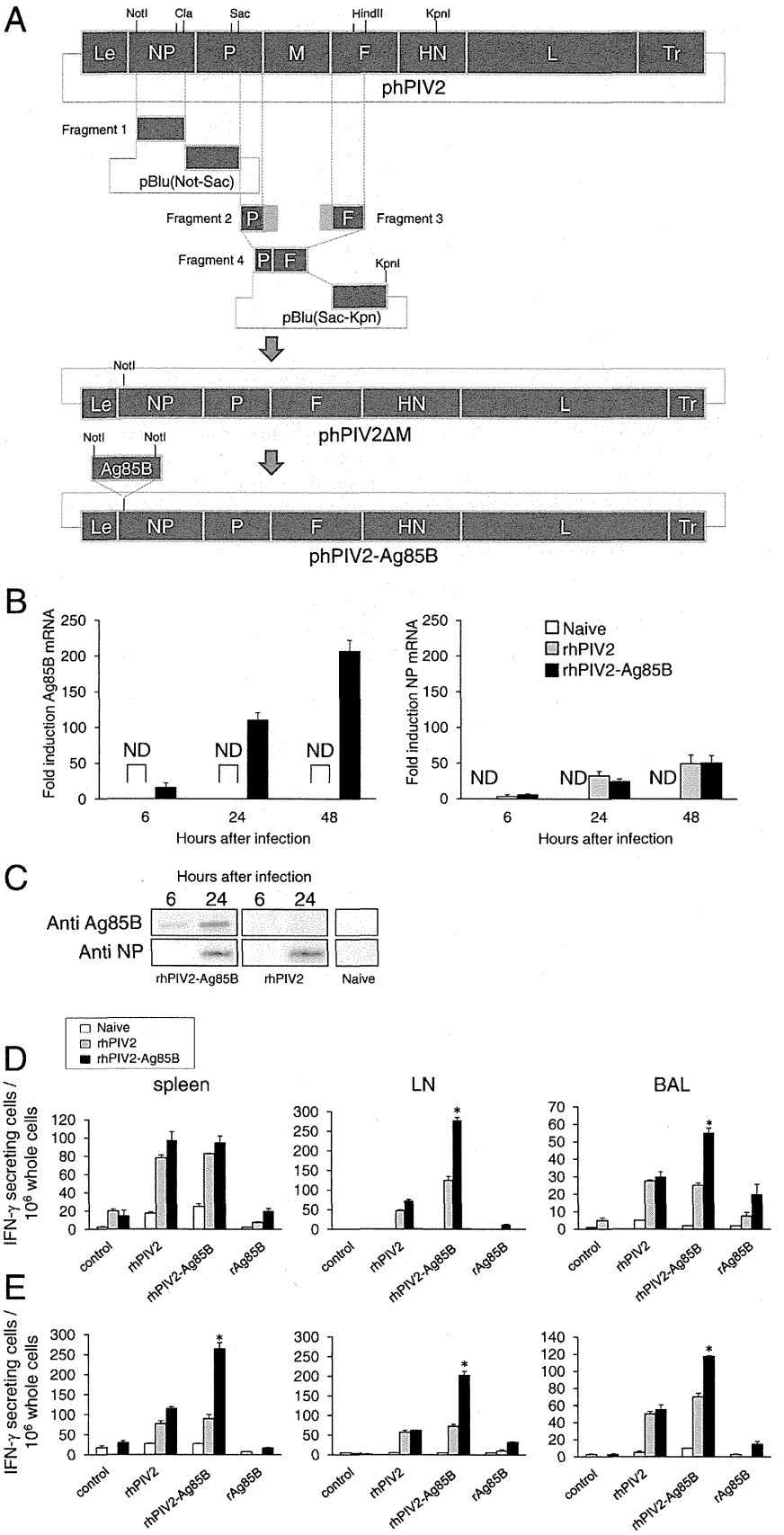

Fig. 1. Expression of Ag85B and advantageous effects in cellular immune response against Ag85B *versus* virus vector in immunized mice. (A) Construction of rhPIV2–Ag85B. (B) Expression of Ag85B (left panel) and NP (right panel) gene in BEAS cells infected with rhPIV2 or rhPIV2–Ag85B at each time point was determined by real-time PCR. Total RNA was extracted at 6, 24, and 48 h after infection. Fold increase of each target gene was normalized to β-actin, and the expression levels are represented as relative values to naïve cells. Error bars represent standard deviation. ND indicates non-detected. (C) Expression of Ag85B and NP proteins was detected by anti-Ag85B and anti-NP antibodies at 6 and 24 h after infection, respectively. (D and E) Mice were immunized 1 (D) or 2 (E) times with rhPIV2 or rhPIV2–Ag85B at a 2-week interval by intranasal

Mycobacterium bovis bacille Calmette-Guérin (BCG) has substantially contributed to the control of tuberculosis (TB) for more than 80 years and affords about 80% protection against tuberculosis meningitis and miliary tuberculosis in infant and young children. However, it is well known that the protective efficacy of BCG against pulmonary TB in adults is variable and partial [5,6]. Therefore, development of new vaccines is urgently needed for the elimination of TB as a public health threat and should be a major global public health priority.

Many infectious diseases, including TB, initially establish infection on mucosal surfaces. Therefore, the best defense against these predominantly mucosal pathogens is mucosal vaccines that are capable of inducing both systemic and mucosal immunity. However, the mucosal immune system is quite unique and is different from systemic immune responses [7,8]. Mucosal immunization provides mucosal immune responses in all mucosal effector tissues in the concept of a common mucosal immune system [9].

Human parainfluenza type 2 virus (hPIV2) is a member of the genus *Rubulavirus* of the family *Paramyxoviridae* and possesses a single-stranded, nonsegmented and negative-stranded RNA genome. This virus does not have a DNA phase during its life cycle and can avoid genetic modifications. Additionally, this virus becomes replication-incompetent by elimination of some viral genes [10]. Moreover, it is likely to lead to elicit stronger inserted antigen-specific immune responses than vector-specific responses unlike other viral vaccine vectors using inserted antigen expression mechanisms of hPIV2. In the present study, we evaluated the effectiveness of intranasal administration of Ag85B-expressed non-replicating human parainfluenza type 2 virus (rhPIV2–Ag85B), which induces weak immune responses against a viral vector, as a novel mucosal TB vaccine.

2. Materials and methods

2.1. Immunization

Six-week-old BALB/c female mice were immunized with rhPIV2–Ag85B or rhPIV2 control vector 3 or 4 times at 2-week intervals by intranasal inoculation of 1×10^8 TCID50 virus in 20 μl PBS. Another group of mice was intramuscularly immunized twice with Ag85B DNA vaccine [11] and intranasally immunized twice with rhPIV2–Ag85B. As a control group, a group of mice was vaccinated using 1×10^7 CFU of BCG Tokyo by subcutaneous injection.

2.2. Infection assay

Two weeks (rhPIV2–Ag85B-immunized mice) or 6 weeks (BCG-immunized mice) after the final immunization, mice were challenged with *M. tuberculosis* (Mtb) Kurono strain by inhalation. This bacterial preparation and infection assay were performed as previously described [12]. In brief, the mice were infected *via* the airborne route by placing them into the exposure chamber of a Glas-Col aerosol generator. The nebulizer compartment was filled with 5 ml of a suspension containing 10^6 CFU of Kurono strain so that approximately 50 bacteria would be deposited in the lungs of each animal. Eight weeks after Mtb infection, mice were sacrificed and the preventive effects of the vaccine were assessed.

2.3. Cell culture

Human bronchial epithelial cells (BEAS cells) and primary cultured normal human bronchial epithelial (NHBE) cells were obtained from the American Type Culture Collection (Manassas, VA) and Lonza (Walkersville, MD). These cells were grown in bronchial epithelial growth medium containing supplements (Lonza). These cells were infected with rhPIV2 or rhPIV2–Ag85B (MOI of 10) or treated with recombinant Ag85B (10 μg/ml) for 6–48 h in a 37 °C incubator with a 5% CO_2 atmosphere.

2.4. FACS analysis

Spleen, pulmonary lymph node (pLN), and bronchoalveolar lavage (BAL) cells were obtained from immunized mice, and single-cell suspensions were prepared. The cells were incubated with recombinant Ag85B protein (10 μg/ml final concentration) for 4 h in the presence of Brefeldin A at 37 °C with 5% CO_2. The cells were stained for surface markers with anti-CD3 and anti-CD4 (BD Biosciences, San Joes, CA) for 30 min at 4 °C, followed by fixation for 30 min at 4 °C in 2% paraformaldehyde. IFN-γ was detected by staining with anti-IFN-γ (BD Biosciences) for 30 min at 4 °C. Flow cytometry data collection was performed on a FACS Canto II (BD Biosciences). Files were analyzed using FACSDiva Software (BD Biosciences). BEAS cells infected with rhPIV2–Ag85B were stained with anti-ICAM-1 (BioLegend, San Diego, CA) and analyzed as described above.

2.5. Evaluation of Ag85B-specific immune responses by ELISPOT assay

The number of Ag85B-specific, IFN-γ-secreting cells was determined by the ELISPOT assay according to the method reported previously [11]. Triplicate samples of whole, $CD4^+$, and $CD8^+$ T cells (separated by a MACS system) (Miltenyi Biotec, Bergisch Gladbach, Germany) collected from the spleen, pLN, and BAL were plated at 1×10^6 cells/well. These cells were stimulated by addition of 2×10^5 mitomycin C (Sigma–Aldrich, Saint Louis, MO)-treated syngeneic spleen cells infected with recombinant vaccinia virus expressing Ag85B or rhPIV2–Ag85B.

2.6. Statistical analysis

Data are presented as means ± SD. Statistical analyses were performed using the Mann–Whitney *U* test. Statistically significant differences compared with the control are indicated by asterisks.

3. Results

3.1. Characteristics of rhPIV2–Ag85B

A construction of rhPIV2–Ag85B is shown in Fig. 1A. To examine gene expression levels of the inserted Ag85B, BEAS cells were infected with rhPIV2–Ag85B. Abundant and rapid expression of mRNA of Ag85B was observed in BEAS cells infected with rhPIV2–Ag85B compared with the expression of NP mRNA (Fig. 1B). These results were also confirmed by analysis of protein expression (Fig. 1C). The production of Ag85B was earlier than that of NP, which is usually the earliest synthesized protein in hPIV2 infection.

inoculation ($n = 5$ per group). Spleen, pLN, and BAL cells were collected from immunized mice ($n = 5$ per group) 2 weeks after the final immunization for examination by an ELISPOT assay. These isolated cells were stimulated *in vitro* with syngeneic spleen cells infected with control rhPIV2, rhPIV2–Ag85B, or recombinant Ag85B protein (rAg85B) (10 μg/ml final concentration) for 24 h. Error bars represent standard deviations. Statistically significant differences are indicated by asterisks (*, $P < 0.05$ compared to the group stimulated with rhPIV2).

These responses were considered to be advantageous effects in cellular immune response to inserted Ag85B *versus* rhPIV2 vector. To confirm this advantageous response, cells from immunized mice were re-stimulated *in vitro* with syngeneic spleen cells infected with rhPIV2 or rhPIV2–Ag85B. Although responses to both Ag85B and rhPIV2 vector were observed, Ag85B-specific responses were clearly seen, especially in pLN and BAL cells after single immunization (Fig. 1D). After performing immunization twice, Ag85B-specific responses were also seen in spleen cells as booster effects more than responses to the vector virus (Fig. 1E). These results indicated that rhPIV2–Ag85B immunization elicited inserted Ag85B-specific immune responses without being hidden by vector responses.

3.2. Intranasal administration of rhPIV2–Ag85B prevents infection with Mtb in mice

To investigate the ability of intranasal administration of rhPIV2–Ag85B to elicit a protective effect against pulmonary TB, rhPIV2–Ag85B-immunized mice were aerosol-infected with highly pathogenic Mtb kurono strain [13]. One group of mice were intranasally immunized with rhPIV2–Ag85B 4 times at 2-week intervals, and another group of mice were intranasally immunized with rhPIV2–Ag85B twice following intramuscular immunization with Ag85B DNA twice (Fig. 2A). Intranasal administration of rhPIV2–Ag85B resulted in a decreases in granulomatous lesions and inflammatory area. However, there were no apparent histopathological differences, such as infiltrating cell types, between the each group of mice, and these results are similar to the results of another study focusing on TB vaccine [14]. On the other hand, these vaccine effects were clearly seen by staining for acid-fast bacillus. Mice immunized with rhPIV2–Ag85B showed a substantial reduction in the infiltration of bacteria, and this inhibitory effect on bacterial expansion was correlated with the number of rhPIV2–Ag85B intranasal administrations (Fig. 2B). CFU of Mtb in spleens from both groups of immunized mice was also significantly lower than those in mice immunized with the control vector (Fig. 2C). As for a preventive effect on Mtb infection in the lung, the mice immunized with rhPIV2–Ag85B clearly showed a substantial reduction in CFU.

3.3. Ag85B-specific immune response is elicited by rhPIV2–Ag85B administration

The capacity of rhPIV2–Ag85B intranasal immunization to elicit effector cells that recognize endogenously expressed Ag85B was assessed. Spleen, pLN, and BAL cells obtained from immunized mice were re-stimulated *in vitro* with syngeneic spleen cells infected with the recombinant vaccinia virus expressing Ag85B, and endogenously expressed Ag85B-specific cellular immune response was examined by ELISPOT assays. Both $CD4^+$ and $CD8^+$ splenocytes exhibited Ag85B-specific responses, and $CD8^+$ T cells showed much stronger responses than those of $CD4^+$ T cells in splenocytes from mice immunized with rhPIV2–Ag85B (Fig. 3A). Ag85B-specific responses were also seen in both $CD4^+$ and $CD8^+$ T cells at almost the same levels in pLN and BAL cells (Fig. 3B and C).

3.4. Analysis of Ag-specific effector cells and immune responses in pLN cells and the lung

Delayed initial activation of effector cells in lungs has been reported in the case of Mtb infection [15]. To control bacterial expansion in the early phase of infection, rapid Mtb Ag-specific $CD4^+$ T cell responses are required. Thus, we next analyzed recruitment of Ag85B-specific IFN-γ^+ $CD4^+$ T cells in pLN and BAL cells in mice immunized with rhPIV2–Ag85B. Mice were intranasally immunized with rhPIV2–Ag85B or the control vector virus 3 times

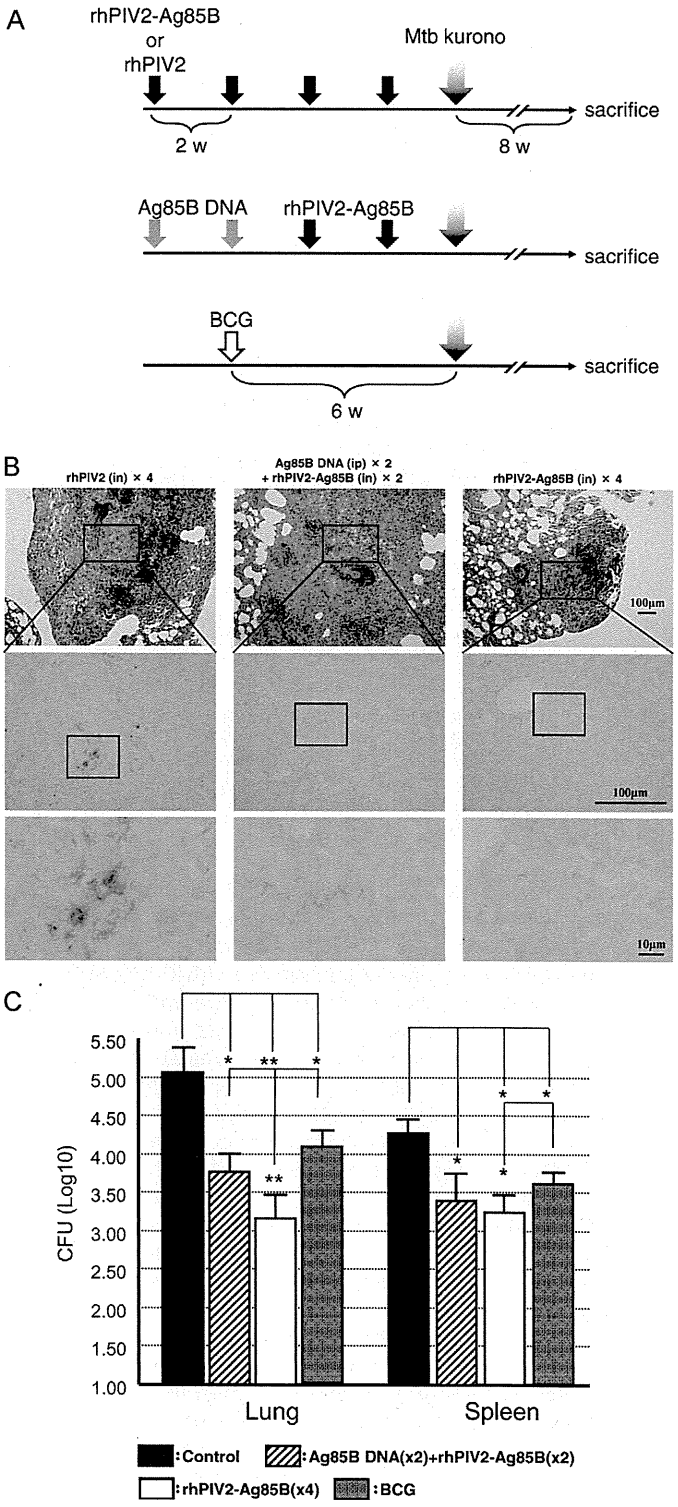

Fig. 2. Repeated immunization with rhPIV2–Ag85B results in protection from TB. (A) Groups of mice were vaccinated in this schedule. (B) Histological images of the lungs of Mtb-infected mice. Groups of mice ($n = 10$) immunized 4 times with rhPIV2 (left panel), 2 times with Ag85B DNA vaccine and 2 times with rhPIV2–Ag85B (middle panel) or 4 times with rhPIV2–Ag85B (right panel) were challenged by Mtb infection. Arrows point to tubercles. Lower panels in (B) show magnified images of images in the middle panels. (C) Inhibition of bacterial growth by immunization with rhPIV2–Ag85B in the lung and spleen. Groups of mice immunized 2 times with Ag85B DNA vaccine and 2 times with rhPIV2–Ag85B or immunized 4 times with rhPIV2–Ag85B or BCG were challenged by Mtb infection. The numbers of Mtb CFU in the lung and spleen were determined by a colony enumeration assay. The bacterial load is represented as mean $\log_{10}$ CFU per organ. Error bars represent standard deviations. Statistically significant differences are indicated by asterisks (*, $P < 0.05$, **, $P < 0.005$).

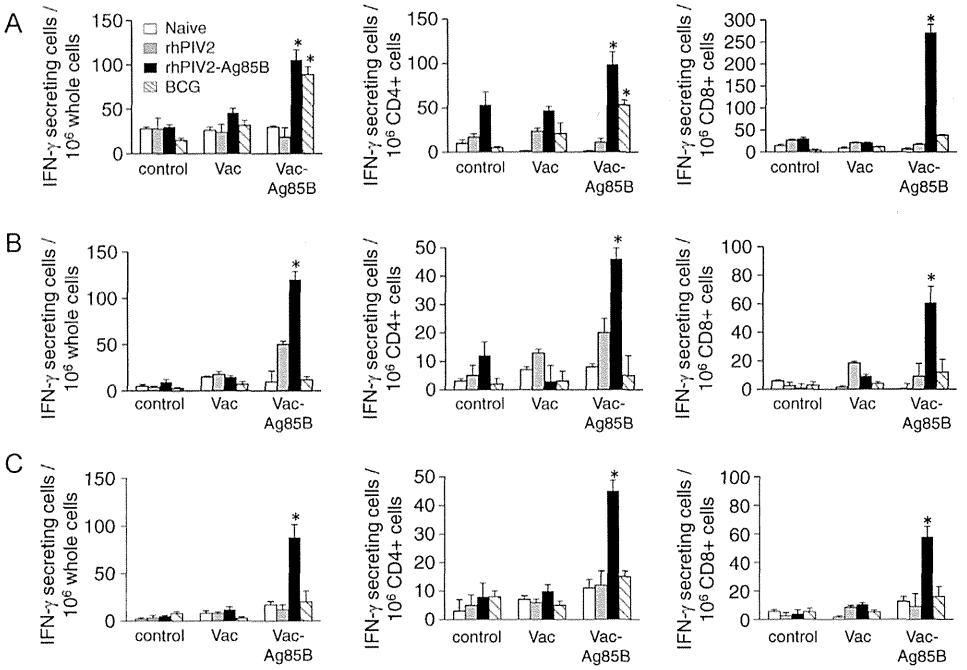

Fig. 3. Induction of Ag85B-specific cellular immune responses in rhPIV2–Ag85B-immunized mice. Mice were immunized with rhPIV2, rhPIV2–Ag85B, or BCG ($n = 5$ per group) according to the schedule shown in Fig. 2A. Two (rhPIV2 or rhPIV2–Ag85B) or 4 weeks (BCG) after the final immunization, the spleen, pLN, and BAL were collected. Isolated cells from the spleen (A), pLN (B), or BAL (C) were separated into whole (left panels), $CD4^+$ (middle panels), and $CD8^+$ (right panels) T cells and examined for IFN-γ production in an ELISPOT assay. These cells were stimulated *in vitro* with syngeneic spleen cells infected with control vaccinia virus (Vac) or recombinant vaccinia virus carrying the Ag85B gene (Vac-Ag85B) for 24 h. Error bars represent standard deviations. Statistically significant differences are indicated by asterisks (*, $P < 0.01$ compared to the group stimulated with Vac).

at 2-week intervals. Another group of mice were immunized with BCG by subcutaneous injection. Two weeks (rhPIV2–Ag85B-immunized mice) or 6 weeks (BCG-immunized mice) after the final immunization, all mice were challenged with Mtb Kurono strain by inhalation (Fig. 4A). At each time point after immunization or Mtb challenge, the percentage and absolute number of Ag85B-specific IFN-γ^+ $CD4^+$ cells were determined by flow cytometry. Before Mtb challenge, the percentage of IFN-γ^+ $CD4^+$ cells in pLN cells was increased by immunization with rhPIV2–Ag85B but not by BCG immunization (Fig. 4B and C, top). However, a significant increase in IFN-γ^+ $CD4^+$ cells was not detected in BAL cells (Fig. 4B and C, bottom). Interestingly, expansion of IFN-γ^+ $CD4^+$ cells occurred after Mtb challenge in BAL cells more dramatically than that in pLN cells in terms of absolute number (Fig. 4C). These responses induced by rhPIV2–Ag85B immunization were much stronger than those induced by BCG immunization.

Similarly, an increase in Ag85B-specific responses was observed by the ELISPOT assay (Fig. 4D). The number of Ag85B-specific IFN-γ secreting cells increased in pLN cells from mice immunized with rhPIV2–Ag85B in a number of immunizations-dependent manner. Furthermore, strong Ag85B-specific responses were detected after Mtb challenge in pLN and BAL cells, and the responses were much stronger than those in BCG immunized mice.

3.5. *rhPIV2–Ag85B induces innate immune responses*

We explored innate immune responses induced by rhPIV2–Ag85B infection. We confirmed that Ag85B did not affect the viability of rhPIV2–Ag85B infected cells (Supplemental Fig. 1) [44–46]. Type I IFNs were assessed after infection with rhPIV2–Ag85B in NHBE and BEAS cells as an indication of innate immune responses. Both types of cells showed mRNA expression of type I IFNs after infection with rhPIV2–Ag85B but not after addition of recombinant Ag85B protein (Fig. 5A). Production of IFN-β was also detected in the culture supernatant by ELISA (Fig. 5B). The mRNA expression of intracellular receptors, RIG-I, MDA5, and TLR3, and the induction of cytokines, IL-6 and IL-15 were also enhanced by infection with rhPIV2–Ag85B, whereas these effects were not observed with the addition of recombinant Ag85B protein (Fig. 5C and D). Furthermore, the expression of ICAM-1 was induced by infection with rhPIV2–Ag85B (Fig. 5E). Similar results were obtained after infection with rhPIV2 vector alone or rhPIV2-GFP (Supplemental Fig. 2). Other co-stimulation molecules, CD80, CD86, ICAM-2 and selectin, were not detected (data not shown).

To further investigate the participation of these receptors in innate immune activation induced by rhPIV2–Ag85B infection, expression of these receptors was knocked down by transfecting siRNA. At 48 h after transfection with siRNA, expression levels of these receptors were reduced by approximately 90% or expression was no longer detectable (Fig. 5F). IFN-β production induced by rhPIV2–Ag85B infection was inhibited when the cells were treated with RIG-I siRNA. For other receptors, MDA5 and TLR3, siRNA treatment did not result in inhibition of IFN-β production induced by rhPIV2–Ag85B infection (Fig. 5G). This result was confirmed by phosphorylation of IRF3, which is a downstream molecule of RIG-I in epithelial cells. The phosphorylation of IRF3 induced by rhPIV2–Ag85B infection was inhibited when epithelial cells were treated with siRNA of RIG-I (Fig. 5H).

4. Discussion

In the present study, we demonstrated the effectiveness of hPIV2 vectors for TB vaccines to induce systemic and mucosal immune responses. The rhPIV2 vector is a weak immunogenic; however, intranasal immunization with rhPIV2–Ag85B showed more potent protection against pulmonary TB in BALB/c mice than did conventional BCG vaccination. The rhPIV2–Ag85B shows a vaccine effect by itself alone, and this effect is more useful than the effects of other vectors for TB vaccines.

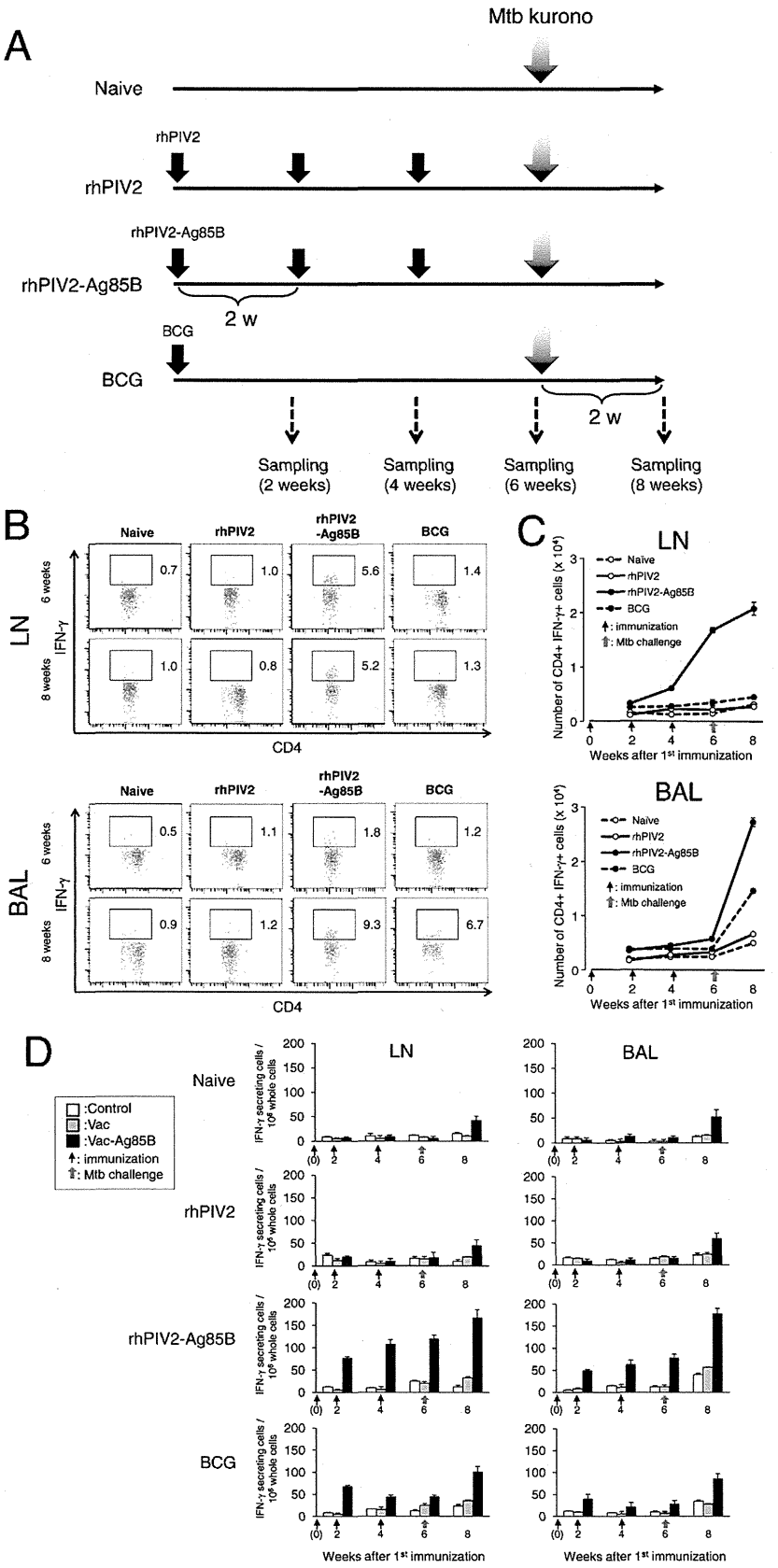

Fig. 4. Analysis of Ag-specific effector cells and these immune responses in pLN and BAL. (A) Groups of mice were immunized with rhPIV2, rhPIV2–Ag85B, or BCG ($n = 10$ per group) and challenged by Mtb infection in this schedule. (B) Representative flow cytometry plots of IFN-γ^+ cells on gated CD4$^+$ cells from pLN (top panels) and BAL (bottom panels) are shown. Numbers shown beside the gates represent the percentages within CD4$^+$ T cells. (C) Kinetics of recruitment of Ag85B-specific IFN-γ^+ cells in pLN (top panel) and BAL (bottom panel). Absolute numbers of IFN-γ^+ CD4$^+$ cell populations at each time points are shown. Error bars represent standard deviations. (D) Isolated cells from the pLN and BAL at each time point were examined for IFN-γ production in an ELISPOT assay. These cells were stimulated *in vitro* with syngeneic spleen cells infected with control vaccinia virus (Vac) or recombinant vaccinia virus carrying the Ag85B gene (Vac-Ag85B) for 24 h. Error bars represent standard deviations.

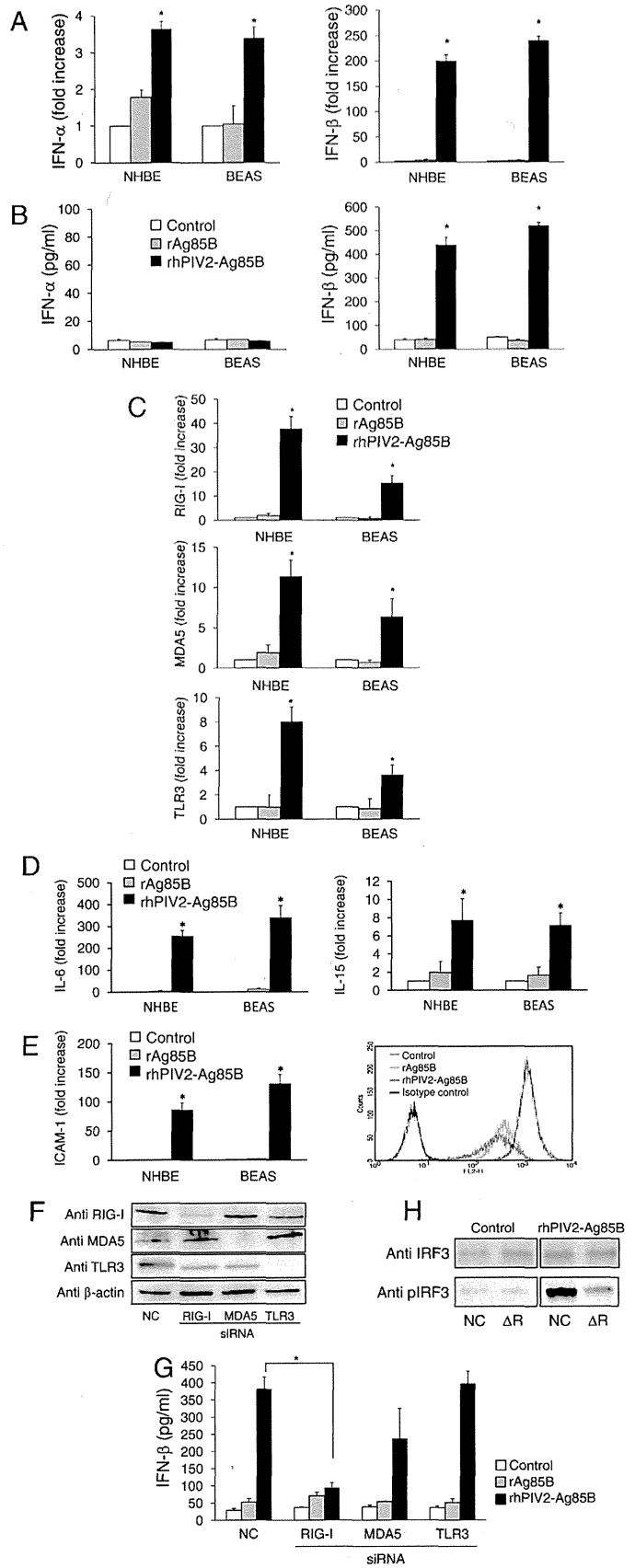

Fig. 5. Evaluation of adjuvant activity of rhPIV2–Ag85B *in vitro*. NHBE and BEAS cells were treated with rAg85B protein (10 μg/ml) or infected with rhPIV2–Ag85B (MOI of 10) for 24 h, and the increases in mRNA levels of IFN-α, IFN-β (A), RIG-I, MDA5, TLR3 (C), IL-6, IL-15 (D), and ICAM-1 (E, left panel) were determined by real-time PCR. Fold increase of each target gene was normalized to β-actin, and the expression levels are represented as relative values to the control. Culture supernatants were also collected, and amounts of secreted IFN-α and IFN-β were measured by ELISA (B). Expression of ICAM-1 was also confirmed by FACS analysis in BEAS cells (E, right panel). Data are averages of triplicate samples from three identical experiments, and error bars represent standard deviations. Statistically significant differences between control cells and rhPIV2–Ag85B-infected cells are indicated by asterisks (*, $P < 0.01$). BEAS cells were treated with siRNA targeting RIG-I, MDA5, TLR3, or the negative control siRNA (NC) for 48 h. Depletion of them was examined by immunoblotting (F). Those cells were stimulated by rAg85B protein (10 μg/ml) or infected with rhPIV2–Ag85B (MOI of 10) and then production of IFN-β was measured by ELISA (G). Data are averages of triplicate samples from three identical experiments, and error bars represent standard deviations. Statistically significant differences are indicated by asterisks (*, $P < 0.01$ compared to NC). The effects of depletion of RIG-I on IRF3 phosphorylation were tested. BEAS cells treated with NC or siRNA targeting RIG-I (ΔR) for 48 h were infected with rhPIV2–Ag85B or not infected (control). Whole IRF3 and phosphorylated IRF3 (pIRF3) were detected by immunoblotting 6 h after infection (H).

Viral vectors are promising vaccine candidates for eliciting Ag-specific immune responses [16,17]. Pre-existing anti-vector antibodies, however, constitute an obstacle for use in humans [18–20]. Although antibodies against hPIV are known to cross-react with Sendai virus, Sendai virus vector is considered to be effective for human use by intranasal administration [21]. Additionally, Sendai virus vector is not affected by antibodies against Sendai virus for induction of T cell responses, especially when it is administered intranasally [4]. From these findings, intranasal administration of the hPIV2 vector is also considered to be effective for human use. In fact, multiple administrations with rhPIV2–Ag85B also showed preventive effects more clearly than did immunization 2 times with rhPIV2–Ag85B (Fig. 2).

Many viral vectors have been tested as recombinant viral vaccines eliciting suitable recombinant Ag-specific immune responses, and many of these vaccine vectors are not vaccine viruses such as vaccinia virus Ankara (MVA), adenovirus, Sendai virus, and CMV. These viral vectors have also been used in several vaccine trials in TB or HIV vaccine [22–24]. Experience in the HIV vaccine field has emphasized the importance of avoiding anti-vector immune responses when developing a vectored vaccine [25]. Immune responses to vaccine vectors prevent the induction of aimed immune responses against recombinant Ag. From these findings, elimination of the immunogenicity of a vaccine vector is critical for a recombinant viral vaccine. The immunogenicity of viral vectors depends on the amount of vector viral proteins. Approximately 80 poxvirus proteins are encoded by its over 130–300 kbp and the adenovirus genome sizes are 26–45 kbp. The genome sizes of these two viral vectors are much larger than that of hPIV2 (15.65 kbp), and induction of immune responses to hPIV2 vector might be lower than other viral vectors. In TB vaccines, recombinant vaccinia virus and adenovirus, which are immunogenic viruses, did not show clear vaccine effects against TB infection by immunization with themselves alone. These two recombinant TB vaccines, adenovirus and MVA, were utilized as boost immunization after BCG priming [26,27]. These heterologous prime-boost strategies diminish immune responses to the vector virus and indicate the possibility of a practical and efficient strategy for prevention of TB [28,29]. On the other hand, the most common method for obtaining an attenuated virus is gene elimination of the viral construct protein to make a replication-deficient virus *in vivo*. The rhPIV2 vector is a weak immunogenicity by elimination of structural protein (M) gene; however, the rhPIV2–Ag85B shows a vaccine effect by immunization with itself alone, and this effect is more useful than the effects of other vectors for a recombinant TB vaccine.

The hPIV2 vector has an additional advantage over other viral vectors. The inserted Ag85B gene, which is only 978 bp, is a minor component of rhPIV2–Ag85B. Despite that, the cellular immune response against Ag85B had an advantage over that against the virus vector in mice. This advantageous effect is thought to depend

on Ag85B expression mechanisms. The frequency with which viral RNA polymerase reinitiates the next mRNA at gene junctions is imperfect, and this leads to a gradient of mRNA abundance that decreases according to distance from the genome 3′ end [30]. Insertion of the Ag85B gene into the 3′ proximal first locus between the leader sequence and the NP gene results in the highest level of gene expression. Ag85B is transcribed earlier and more abundantly than other viral products (Fig. 1B and C). This property of rhPIV2–Ag85B leads to elicit stronger Ag85B-specific immune responses than vector-specific responses in our system (Fig. 1D and E), although recombinant virus vaccine immunization usually induces overwhelming viral-specific immune responses compared with an inserted gene product [31,32]. We also demonstrated that intranasal administration of the rhPIV2 vector had no adverse effects and provided sufficient immunogenicity and a sufficient vaccine effect against Mtb in mice. These results suggest that intranasal administration of rhPIV2–Ag85B does not cause functional failure as a vaccine by multiple administrations, and these features of the rhPIV2 vector are definitely advantages for clinical use.

Another major feature of rhPIV2–Ag85B is effective prevention of TB by intranasal administration. Vaccination in the respiratory tract may enhance protection against Mtb infection, since Mtb initially establishes infection on mucosal surfaces of the respiratory tract. Indeed, a number of recombinant TB vaccines have been developed and evaluated for respiratory mucosal immunization [33–35]. It is important to note that lack of Ag-specific effector cells persists even up to about 21 days after pulmonary Mtb infection caused by a bacterial component [15,36]. In the present study, the arrival of Ag-specific T cells was detected in lung and pLN by rhPIV2–Ag85B immunization, and this arrival of effector cells was recognized faster than BCG immunization after Mtb challenge (Fig. 4B and C). We were able to establish a novel intranasal vaccine, rhPIV2–Ag85B, against TB by utilizing various advantages of intranasal administration. Nasal administration of a vaccine to induce mucosal and systemic immune responses has several advantages other than the induction of effective immune responses. It is even possible that intranasal administration of replication-incompetent rhPIV2–Ag85B limits the areas of infection in respiratory organs and induces a respiratory tract mucosal immune response in addition to a systemic immune response against TB. Our study suggested that intranasal administration of rhPIV2–Ag85B, which can induce both mucosal and systemic immune responses against Mtb, has a great advantage as a TB vaccine.

Attempts have been made to use various types of adjuvants for enhancing an immune responses to vaccines, including vaccines against TB [37]. In fact, a protein-based TB vaccine required the addition of an adjuvant to induce effective immune responses [38–41]. For the generation of adaptive immune responses, induction of innate immunity is crucial for vaccines to elicit potent Ag-specific immune responses. Pattern recognition receptors have been studied as potential targets for an adjuvant. dsRNA is a dominant activator of innate immunity because viral dsRNA is recognized by TLR3, RIG-I, and MDA5 [42,43]. As a result, it was demonstrated that the rhPIV2 vector had a potent adjuvant activity as dsRNA recognized by the RIG-I receptor and enhanced not only local innate immunity but also systemic adaptive immunity. It is possible that no extra addition of an adjuvant is required to prevent TB by vaccination with rhPIV2–Ag85B. Furthermore, the inhibitory effects on the growth of rhPIV2–Ag85B *in vivo* by IFN through the innate receptor are not required to consider since the rhPIV2 vector is replication-incompetent *in vivo* by elimination of the M gene (Fig. 1A).

In summary, our results provide evidence for the possibility of rhPIV2–Ag85B as a novel intranasal vaccine for eliciting Mtb-specific mucosal immunity. Immunization with rhPIV2–Ag85B showed significant protection against TB without any prime vaccine or addition of an adjuvant in mice. Further studies will contribute to the ultimate goal of establishing a new vaccine strategy that can definitely prevent Mtb infection.

Acknowledgements

We thank members of AERAS for helpful advice and Dr. Yasuhiko Ito (Chubu University, Japan) and Dr. Isamu Sugawara (The Research Institute of Tuberculosis) for useful suggestion. This work was supported by Health Science Research Grants from the Ministry of Health, Labor and Welfare of Japan and the Ministry of Education, Culture, Sports, Science and Technology of Japan. This work was also supported by a grant from the Cooperative Link of Unique Science and Technology for Economy Revitalization (CLUSTER) promoted by the Ministry of Education, Culture, Sports and Technology, Japan.

Appendix A. Supplementary data

Supplementary material related to this article can be found, in the online version, at http://dx.doi.org/10.1016/j.vaccine.2013.11.108.

References

[1] Small JC, Ertl HC. Viruses – from pathogens to vaccine carriers. Curr Opin Virol 2011;1(October (4)):241–5.
[2] Halle S, Dujardin HC, Bakocevic N, Fleige H, Danzer H, Willenzon S, et al. Induced bronchus-associated lymphoid tissue serves as a general priming site for T cells and is maintained by dendritic cells. J Exp Med 2009;206(November (12)):2593–601.
[3] Okano S, Yonemitsu Y, Shirabe K, Kakeji Y, Maehara Y, Harada M, et al. Provision of continuous maturation signaling to dendritic cells by RIG-I-stimulating cytosolic RNA synthesis of Sendai virus. J Immunol 2011;186(February (3)):1828–39.
[4] Moriya C, Horiba S, Kurihara K, Kamada T, Takahara Y, Inoue M, et al. Intranasal Sendai viral vector vaccination is more immunogenic than intramuscular under pre-existing anti-vector antibodies. Vaccine 2011;29(November (47)):8557–63.
[5] Randomised controlled trial of single BCG, repeated BCG, or combined BCG and killed *Mycobacterium leprae* vaccine for prevention of leprosy and tuberculosis in Malawi. Karonga Prevention Trial Group. Lancet 1996;348(July (9019)):17–24.
[6] Rodrigues LC, Pereira SM, Cunha SS, Genser B, Ichihara MY, de Brito SC, et al. Effect of BCG revaccination on incidence of tuberculosis in school-aged children in Brazil: the BCG-REVAC cluster-randomised trial. Lancet 2005;366(October (9493)):1290–5.
[7] Zinselmeyer BH, Dempster J, Gurney AM, Wokosin D, Miller M, Ho H, et al. In situ characterization of CD4+ T cell behavior in mucosal and systemic lymphoid tissues during the induction of oral priming and tolerance. J Exp Med 2005;201(June (11)):1815–23.
[8] Dwivedy A, Aich P. Importance of innate mucosal immunity and the promises it holds. Int J Gen Med 2011;4:299–311.
[9] Kiyono H, Kweon MN, Hiroi T, Takahashi I. The mucosal immune system: from specialized immune defense to inflammation and allergy. Acta Odontol Scand 2001;59(June (3)):145–53.
[10] Kawano M, Kaito M, Kozuka Y, Komada H, Noda N, Nanba K, et al. Recovery of infectious human parainfluenza type 2 virus from cDNA clones and properties of the defective virus without V-specific cysteine-rich domain. Virology 2001;284(May (1)):99–112.
[11] Takamura S, Matsuo K, Takebe Y, Yasutomi Y. Ag85B of mycobacteria elicits effective CTL responses through activation of robust Th1 immunity as a novel adjuvant in DNA vaccine. J Immunol 2005;175(August (4)):2541–7.
[12] Sugawara I, Mizuno S, Yamada H, Matsumoto M, Akira S. Disruption of nuclear factor-interleukin-6, a transcription factor, results in severe mycobacterial infection. Am J Pathol 2001;158(February (2)):361–6.
[13] Sugawara I, Yamada H, Kazumi Y, Doi N, Otomo K, Aoki T, et al. Induction of granulomas in interferon-gamma gene-disrupted mice by avirulent but not by virulent strains of *Mycobacterium tuberculosis*. J Med Microbiol 1998;47(October (10)):871–7.
[14] Sweeney KA, Dao DN, Goldberg MF, Hsu T, Venkataswamy MM, Henao-Tamayo M, et al. A recombinant *Mycobacterium smegmatis* induces potent bactericidal immunity against *Mycobacterium tuberculosis*. Nat Med 2011;17(October (10)):1261–8.

[15] Shafiani S, Tucker-Heard G, Kariyone A, Takatsu K, Urdahl KB. Pathogen-specific regulatory T cells delay the arrival of effector T cells in the lung during early tuberculosis. J Exp Med 2010;207(July (7)):1409–20.
[16] Draper SJ, Heeney JL. Viruses as vaccine vectors for infectious diseases and cancer. Nat Rev Microbiol 2010;8(January (1)):62–73.
[17] Clark KR, Johnson PR. Gene delivery of vaccines for infectious disease. Curr Opin Mol Ther 2001;3(August (4)):375–84.
[18] Sumida SM, Truitt DM, Lemckert AA, Vogels R, Custers JH, Addo MM, et al. Neutralizing antibodies to adenovirus serotype 5 vaccine vectors are directed primarily against the adenovirus hexon protein. J Immunol 2005;174(June (11)):7179–85.
[19] Catanzaro AT, Koup RA, Roederer M, Bailer RT, Enama ME, Moodie Z, et al. Phase 1 safety and immunogenicity evaluation of a multiclade HIV-1 candidate vaccine delivered by a replication-defective recombinant adenovirus vector. J Infect Dis 2006;194(December (12)):1638–49.
[20] Priddy FH, Brown D, Kublin J, Monahan K, Wright DP, Lalezari J, et al. Safety and immunogenicity of a replication-incompetent adenovirus type 5 HIV-1 clade B gag/pol/nef vaccine in healthy adults. Clin Infect Dis 2008;46(June (11)):1769–81.
[21] Hara H, Hironaka T, Inoue M, Iida A, Shu T, Hasegawa M, et al. Prevalence of specific neutralizing antibodies against Sendai virus in populations from different geographic areas: implications for AIDS vaccine development using Sendai virus vectors. Hum Vaccin 2011;7(June (6)):639–45.
[22] McShane H, Brookes R, Gilbert SC, Hill AV. Enhanced immunogenicity of CD4(+) t-cell responses and protective efficacy of a DNA-modified vaccinia virus Ankara prime-boost vaccination regimen for murine tuberculosis. Infect Immun 2001;69(February (2)):681–6.
[23] Radosevic K, Wieland CW, Rodriguez A, Weverling GJ, Mintardjo R, Gillissen G, et al. Protective immune responses to a recombinant adenovirus type 35 tuberculosis vaccine in two mouse strains: CD4 and CD8 T-cell epitope mapping and role of gamma interferon. Infect Immun 2007;75(August (8)):4105–15.
[24] Munier CM, Andersen CR, Kelleher AD. HIV vaccines: progress to date. Drugs 2011;71(March (4)):387–414.
[25] Cheng C, Wang L, Gall JG, Nason M, Schwartz RM, McElrath MJ, et al. Decreased pre-existing Ad5 capsid and Ad35 neutralizing antibodies increase HIV-1 infection risk in the Step trial independent of vaccination. PLoS ONE 2012;7(4):e33969.
[26] Abel B, Tameris M, Mansoor N, Gelderbloem S, Hughes J, Abrahams D, et al. The novel tuberculosis vaccine, AERAS-402, induces robust and polyfunctional CD4+ and CD8+ T cells in adults. Am J Respir Crit Care Med 2010;181(June (12)):1407–17.
[27] McShane H, Pathan AA, Sander CR, Keating SM, Gilbert SC, Huygen K, et al. Recombinant modified vaccinia virus Ankara expressing antigen 85A boosts BCG-primed and naturally acquired antimycobacterial immunity in humans. Nat Med 2004;10(November (11)):1240–4.
[28] Rahman S, Magalhaes I, Rahman J, Ahmed RK, Sizemore DR, Scanga CA, et al. Prime-boost vaccination with rBCG/rAd35 enhances CD8(+) cytolytic T-cell responses in lesions from *Mycobacterium tuberculosis*-infected primates. Mol Med 2012;18:647–58.
[29] Pathan AA, Minassian AM, Sander CR, Rowland R, Porter DW, Poulton ID, et al. Effect of vaccine dose on the safety and immunogenicity of a candidate TB vaccine, MVA85A, in BCG vaccinated UK adults. Vaccine 2012;30(August (38)):5616–24.
[30] Tokusumi T, Iida A, Hirata T, Kato A, Nagai Y, Hasegawa M. Recombinant Sendai viruses expressing different levels of a foreign reporter gene. Virus Res 2002;86(June (1–2)):33–8.
[31] Sakurai H, Kawabata K, Sakurai F, Nakagawa S, Mizuguchi H. Innate immune response induced by gene delivery vectors. Int J Pharm 2008;354(April (1–2)):9–15.
[32] Chen D, Murphy B, Sung R, Bromberg JS. Adaptive and innate immune responses to gene transfer vectors: role of cytokines and chemokines in vector function. Gene Ther 2003;10(June (11)):991–8.
[33] Wang J, Thorson L, Stokes RW, Santosuosso M, Huygen K, Zganiacz A, et al. Single mucosal, but not parenteral, immunization with recombinant adenoviral-based vaccine provides potent protection from pulmonary tuberculosis. J Immunol 2004;173(November (10)):6357–65.
[34] Dietrich J, Andersen C, Rappuoli R, Doherty TM, Jensen CG, Andersen P. Mucosal administration of Ag85B-ESAT-6 protects against infection with *Mycobacterium tuberculosis* and boosts prior bacillus Calmette-Guerin immunity. J Immunol 2006;177(November (9)):6353–60.
[35] Ballester M, Nembrini C, Dhar N, de Titta A, de Piano C, Pasquier M, et al. Nanoparticle conjugation and pulmonary delivery enhance the protective efficacy of Ag85B and CpG against tuberculosis. Vaccine 2011;29(September (40)):6959–66.
[36] Wolf AJ, Desvignes L, Linas B, Banaiee N, Tamura T, Takatsu K, et al. Initiation of the adaptive immune response to *Mycobacterium tuberculosis* depends on antigen production in the local lymph node, not the lungs. J Exp Med 2008;205(January (1)):105–15.
[37] Moreno-Mendieta SA, Rocha-Zavaleta L, Rodriguez-Sanoja R. Adjuvants in tuberculosis vaccine development. FEMS Immunol Med Microbiol 2010;58(February (1)):75–84.
[38] Lin PL, Dietrich J, Tan E, Abalos RM, Burgos J, Bigbee C, et al. The multistage vaccine H56 boosts the effects of BCG to protect cynomolgus macaques against active tuberculosis and reactivation of latent *Mycobacterium tuberculosis* infection. J Clin Invest 2012;122(January (1)):303–14.
[39] Aagaard C, Hoang T, Dietrich J, Cardona PJ, Izzo A, Dolganov G, et al. A multistage tuberculosis vaccine that confers efficient protection before and after exposure. Nat Med 2011;17(February (2)):189–94.
[40] Bertholet S, Ireton GC, Ordway DJ, Windish HP, Pine SO, Kahn M, et al. A defined tuberculosis vaccine candidate boosts BCG and protects against multidrug-resistant *Mycobacterium tuberculosis*. Sci Transl Med 2010;2(October (53)):53ra74.
[41] Von Eschen K, Morrison R, Braun M, Ofori-Anyinam O, De Kock E, Pavithran P, et al. The candidate tuberculosis vaccine Mtb72F/AS02A: tolerability and immunogenicity in humans. Hum Vaccine 2009;5(July (7)):475–82.
[42] Alexopoulou L, Holt AC, Medzhitov R, Flavell RA. Recognition of double-stranded RNA and activation of NF-kappaB by Toll-like receptor 3. Nature 2001;413(October (6857)):732–8.
[43] Kato H, Takeuchi O, Sato S, Yoneyama M, Yamamoto M, Matsui K, et al. Differential roles of MDA5 and RIG-I helicases in the recognition of RNA viruses. Nature 2006;441(May (7089)):101–5.
[44] Buchholz UJ, Finke S, Conzelmann KK. Generation of bovine respiratory syncytial virus (BRSV) from cDNA: BRSV NS2 is not essential for virus replication in tissue culture, and the human RSV leader region acts as a functional BRSV genome promoter. J Virol 1999;73(January (1)):251–9.
[45] Yasui F, Kai C, Kitabatake M, Inoue S, Yoneda M, Yokochi S, et al. Prior immunization with severe acute respiratory syndrome (SARS)-associated coronavirus (SARS-CoV) nucleocapsid protein causes severe pneumonia in mice infected with SARS-CoV. J Immunol 2008;181(November (9)):6337–48.
[46] Falkner FG, Moss B. *Escherichia coli* gpt gene provides dominant selection for vaccinia virus open reading frame expression vectors. J Virol 1988;62(June (6)):1849–54.

Nonagonistic Dectin-1 ligand transforms CpG into a multitask nanoparticulate TLR9 agonist

Kouji Kobiyama[a,b], Taiki Aoshi[a,b], Hirotaka Narita[c], Etsushi Kuroda[a,b], Masayuki Hayashi[a,b], Kohhei Tetsutani[a,b], Shohei Koyama[d,e], Shinichi Mochizuki[f], Kazuo Sakurai[f], Yuko Katakai[g], Yasuhiro Yasutomi[h], Shinobu Saijo[i,j], Yoichiro Iwakura[k], Shizuo Akira[l], Cevayir Coban[m], and Ken J. Ishii[a,b,1]

[a]Laboratory of Adjuvant Innovation, National Institute of Biomedical Innovation, Osaka 567-0085, Japan; Laboratories of [b]Vaccine Science, [l]Host Defense, and [m]Malaria Immunology, World Premier International Immunology Frontier Research Center and [c]Supramolecular Crystallography, Research Center for Structural and Functional Proteomics, Institute for Protein Research, Osaka University, Osaka 565-0871, Japan; [d]Department of Medical Oncology and [e]Cancer Vaccine Center, Dana-Farber Cancer Institute, Boston, MA 02115; [f]Department of Chemistry and Biochemistry, University of Kitakyushu, Fukuoka 808-0135, Japan; [g]Corporation for Production and Research of Laboratory Primates, Ibaraki 305-0843, Japan; [h]Tsukuba Primate Research Center, National Institute of Biomedical Innovation, Ibaraki 305-0843, Japan; [i]Department of Molecular Immunology, Medical Mycology Research Center, Chiba University, Chiba 260-8673, Japan; [j]Precursory Research for Embryonic Science and Technology, Japan Science and Technology Agency, Saitama 332-0012, Japan; and [k]Division of Experimental Animal Immunology, Research Institute for Biomedical Sciences, Tokyo University of Science, Chiba 278-8510, Japan

Edited by Rafi Ahmed, Emory University, Atlanta, GA, and approved January 16, 2014 (received for review October 12, 2013)

CpG DNA, a ligand for Toll-like receptor 9 (TLR9), has been one of the most promising immunotherapeutic agents. Although there are several types of potent humanized CpG oligodeoxynucleotide (ODN), developing "all-in-one" CpG ODNs activating both B cells and plasmacytoid dendritic cells forming a stable nanoparticle without aggregation has not been successful. In this study, we generated a novel nanoparticulate K CpG ODN (K3) wrapped by the nonagonistic Dectin-1 ligand schizophyllan (SPG), K3-SPG. In sharp contrast to K3 alone, K3-SPG stimulates human peripheral blood mononuclear cells to produce a large amount of both type I and type II IFN, targeting the same endosome where IFN-inducing D CpG ODN resides without losing its K-type activity. K3-SPG thus became a potent adjuvant for induction of both humoral and cellular immune responses, particularly CTL induction, to coadministered protein antigens without conjugation. Such potent adjuvant activity of K3-SPG is attributed to its nature of being a nanoparticle rather than targeting Dectin-1 by SPG, accumulating and activating antigen-bearing macrophages and dendritic cells in the draining lymph node. K3-SPG acting as an influenza vaccine adjuvant was demonstrated in vivo in both murine and nonhuman primate models. Taken together, K3-SPG may be useful for immunotherapeutic applications that require type I and type II IFN as well as CTL induction.

innate immunity | two-photon microscopy | MARCO | Siglec-1 | β-glucan

CpG oligodeoxynucleotide (CpG ODN) is a short (~20 bases), single-stranded synthetic DNA fragment containing the immunostimulatory CpG motif, a potent agonist for Toll-like receptor 9 (TLR9), which activates dendritic cells (DCs) and B cells to produce type I interferons (IFNs) and inflammatory cytokines (1, 2) and acts as an adjuvant toward both Th1-type humoral and cellular immune responses, including cytotoxic T-lymphocyte (CTL) responses (3, 4). Therefore, CpG ODN has been postulated as a possible immunotherapeutic agent against infectious diseases, cancer, asthma, and pollinosis (2, 5).

There are at least four types of CpG ODN, each of which has a different backbone, sequence, and immunostimulatory properties (6). D-type (also called A) CpG ODNs typically comprise one palindromic CpG motif with a phosphodiester (PO) backbone and phosphorothioate (PS) poly(G) tail, and activates plasmacytoid DCs (pDCs) to produce a large amount of IFN-α but fails to induce pDC maturation and B-cell activation (7, 8). The three other types of ODN consist of a PS backbone. K-type (also called B) CpG ODN contains nonpalindromic multiple CpG motifs, and strongly activates B cells to produce IL-6 and pDCs to maturation but barely produces IFN-α (8, 9). Recently, C and P CpG ODNs have been developed; these contain one and two palindromic CpG sequences, respectively, both of which can activate B cells like K-type and pDC like D-type, although C CpG ODN induces weaker IFN-α production compared with P CpG ODN (10–12).

D and P CpG ODNs have been shown to form higher-order structures, Hoogsteen base pairing to form parallel quadruplex structures called G tetrads, and Watson–Crick base pairing between *cis*- and *trans*-palindromic portions, respectively, that are required for robust IFN-α production by pDCs (12–14). Although such higher-order structures appear necessary for localization to early endosomes and signaling via TLR9, they suffer from product polymorphisms, aggregation, and precipitation, thereby hampering their clinical application (15). Therefore, only K and C CpG ODNs are generally available as immunotherapeutic agents and vaccine adjuvants for human use (16, 17). Although K CpG ODN enhances the immunogenicity of vaccines targeting infectious diseases and cancers in human clinical trials (6, 17), chemical or physical conjugation between antigen and K CpG ODN is necessary for optimal adjuvant effects. These results indicate that these four (K, D, P, and C) types of CpG ODN have advantages and disadvantages; however, the

Significance

CpG oligodeoxynucleotide (ODN), a Toll-like receptor 9 ligand, is a promising immunotherapeutic agent; however, developing an IFN-inducing CpG ODN forming a stable nanoparticle without aggregation has been unsuccessful. Here we generated a nanoparticulate CpG ODN (K3) wrapped by the nonagonistic Dectin-1 ligand schizophyllan (SPG), K3-SPG. K3-SPG stimulates human peripheral blood mononuclear cells to produce large amounts of both type I and II IFN. K3-SPG thus became a potent adjuvant, especially for cytotoxic T-lymphocyte (CTL) induction to coadministered protein antigens without conjugation, which is attributable to its nanoparticulate nature rather than to targeting Dectin-1. Protective potency of K3-SPG as an influenza vaccine adjuvant was demonstrated in both murine and nonhuman primate models. K3-SPG may be used as an IFN inducer as well as a CTL inducer for immunotherapeutic applications.

Author contributions: K.K., T.A., C.C., and K.J.I. designed research; K.K., T.A., H.N., M.H., and Y.K. performed research; T.A., H.N., E.K., M.H., K.T., S.M., K.S., Y.K., Y.Y., S.S., Y.I., and S.A. contributed new reagents/analytic tools; K.K., T.A., H.N., E.K., S.K., C.C., and K.J.I. analyzed data; and K.K., T.A., E.K., and K.J.I. wrote the paper.

Conflict of interest statement: K.S. holds a patent related to schizophyllan forming a complex with nucleic acids. K.K., T.A., and K.J.I. have filed a patent application related to the content of this manuscript.

This article is a PNAS Direct Submission.

Freely available online through the PNAS open access option.

[1]To whom correspondence should be addressed. E-mail: kenishii@biken.osaka-u.ac.jp.

This article contains supporting information online at www.pnas.org/lookup/suppl/doi:10.1073/pnas.1319268111/-/DCSupplemental.

development of an "all-in-one" CpG ODN activating both B cells and pDCs that forms a stable nanoparticle without aggregation has yet to be accomplished. A better strategy, targeting CpG ODN toward antigen-presenting cells (APCs), is desired to improve immunostimulatory specificity and immunotherapeutic efficacy of CpG ODNs.

Schizophyllan (SPG), a soluble β-glucan derived from *Schizophyllum commune*, is a drug that has been approved in Japan as an enhancer of radiotherapy in cervical carcinoma patients for the last three decades (18). It has been shown to form a complex with polydeoxyadenylic acid (dA) as a triple-helical structure (19). Although we previously demonstrated that mouse and humanized CpG ODN with PO poly(dA) at the 5′ end complexed with SPG enhanced cytokine production and acted as an influenza vaccine adjuvant (20, 21), it has been difficult to achieve high yields of the CpG–SPG complex toward its more efficient and cost-effective preclinical as well as clinical development. Recently, when the PS backbone of the dA sequence was linked to CpG ODN, the efficacy of complex formation was elevated by nearly 100% (22). However, a thorough investigation has yet to be conducted to identify the best humanized CpG sequence and optimization of factors to gain all-in-one activities of the four types of CpG ODN.

To do this, we sought to optimize a humanized CpG–SPG complex as a vaccine adjuvant and immunostimulatory agent in humans (in vitro), mice (in vitro and in vivo), and nonhuman primates (in vivo). In this study, we identified a novel K CpG ODN (K3) and SPG complex, namely K3-SPG. It forms a higher-order nanoparticle that can be completely solubilized. We found that this all-in-one K3-SPG displayed a more potent activity than, and different characteristics from, any other type of CpG ODN and previous CpG–SPG complexes.

Results

A Rod-Shaped Nano-Sized Particle of K3-SPG Gains Dual Characteristics of K- and D-Type CpG ODNs. To make a complex between CpG ODNs and schizophyllan (SPG), CpG ODNs need additional sequences of phosphorothioate backbone of 40-mer polydeoxyadenylic acid (dA_{40}) at the 5′ or 3′ end (20, 22). Fig. 1*A* shows methods of CpG ODN and SPG complexation through denaturing–renaturing procedures. In this study, we selected K3 as a K-type CpG ODN. At first, we examined the immunostimulatory impacts of the 5′ and 3′ ends of CpG ODN. 5′-K3-dA_{40}-3′, but not 5′-dA_{40}-K3-3′, complexed with SPG-activated human peripheral blood mononuclear cells (PBMCs) to produce a robust amount of IFN-α (Fig. 1*B* and Fig. S1). K3, K3-dA_{40}, or dA_{40}-K3, which are able to activate human PBMCs to produce other cytokines such as IL-6, failed to produce IFN-α (Fig. 1*B* and Fig. S1). These results indicate that the 5′-CpG sequence (K3-SPG) is more desirable than the 3′-CpG sequence as a novel TLR9 agonist. Although some CpG ODN-induced cytokine production is known to have a dose-dependent correlation, K3-SPG–induced IFN-α production is not. Given that previous reports showed that IFN-α pro-duction by K CpG ODN stimulation has a bell-shaped dose–response correlation (7), altogether these results suggest that K3-SPG still has the character of K CpG ODN.

Qualification and quantitation of K3-SPG were conducted by scanning electron microscopy (SEM) and dynamic light scattering (DLS). K3-SPG had a rod-like structure, consistent with that seen in a previous report (23) (Fig. 1*C*). It appeared to be a soluble monomeric nanoparticle with an average diameter of 30 nm, comparable to SPG itself and smaller than D CpG ODN (D35) (14, 24) (Fig. 1*D*). Given that K3-SPG forms a nanoparticle, we compared the immunostimulatory activities of K3-SPG with D, C, and P CpG ODNs. PBMCs stimulated with K3-SPG produced larger amounts of IFN-α and IFN-γ but at far lower concentrations than those induced by D35 (Fig. 1*E*) and P and C CpG ODNs (Fig. S2). These results suggest that K3-SPG gains the characteristic of D CpG ODN without losing that of the K type, because these IFNs are known to be D type-specific cytokines (7, 8, 25). To understand the dual functions of K and D

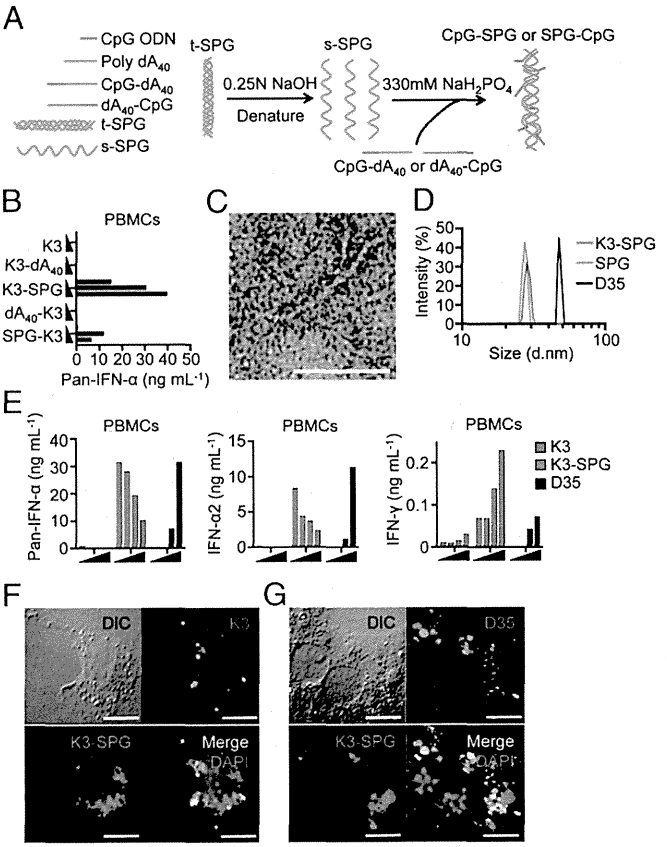

Fig. 1. K (B) CpG ODN and SPG complex forms nanoparticles and gains D (A) CpG ODN characteristics. (*A*) Methods of CpG ODN and SPG complexation. tSPG, triple-stranded SPG; sSPG, single-stranded SPG. (*B*) Production of IFN-α by human PBMCs stimulated with K3, K3-dA_{40}, K3-SPG, dA_{40}-K3, or SPG-K3 (adjusted for K3 ODN concentration at 0.1, 0.3, or 1 μM) for 24 h was measured by ELISA. (C) K3-SPG processed for SEM. (Scale bar, 50 μm.) (*D*) Size of K3-SPG, SPG, and D35 was analyzed by DLS. (*E*) Production of type I and II IFNs by PBMCs stimulated with K3, K3-SPG, or D35 for 24 h was measured by ELISA. (*F* and *G*) Mouse BMDMs were stimulated with Alexa 488-K3 (*F*) or Alexa 488-D35 (*G*) and Alexa 647-K3-SPG at 1 μM for 3 h. The cells were incubated with Hoechst 33258, fixed, and analyzed by fluorescence microscopy. DIC, differential interference contrast. (Scale bars, 10 μm.) Data represent one of three independent experiments with similar results.

CpG ODNs, we analyzed the intracellular localization of K3-SPG in bone marrow-derived macrophages (BMDMs). K3-SPG was colocalized with not only the endosomes containing K CpG ODN but also those containing D CpG ODN (Fig. 1 *F* and *G*) such as C CpG ODN (26), suggesting that K3-SPG may transduce endosome-mediated innate immune signaling pathways by K and D CpG ODNs. These results strongly suggest that K3-SPG forms a nano-sized higher-order and completely solubilized particle and found that this all-in-one K3-SPG displayed a more potent activity than, and different characteristic from, any other CpG ODNs and previously known CpG–SPG complex.

K3-SPG Is a Prominent Vaccine Adjuvant That Induces Potent CTL Responses to Protein Antigen Without Conjugation. We compared the adjuvant effects of K3, K3-dA_{40}, and K3-SPG in a murine immunization model. When wild-type mice were immunized with LPS-free chicken ovalbumin protein (OVA) alone or OVA with each K3-derived adjuvant, K3-SPG induced significantly higher humoral immune responses (Fig. 2*A*) and stronger T-cell responses than that induced by K3 (Fig. 2*B*). Of note, tetramer assays revealed a significantly greater number of OVA-specific CD8 T cells (Fig. 2*C*). We also observed very strong in vivo CTL activity against

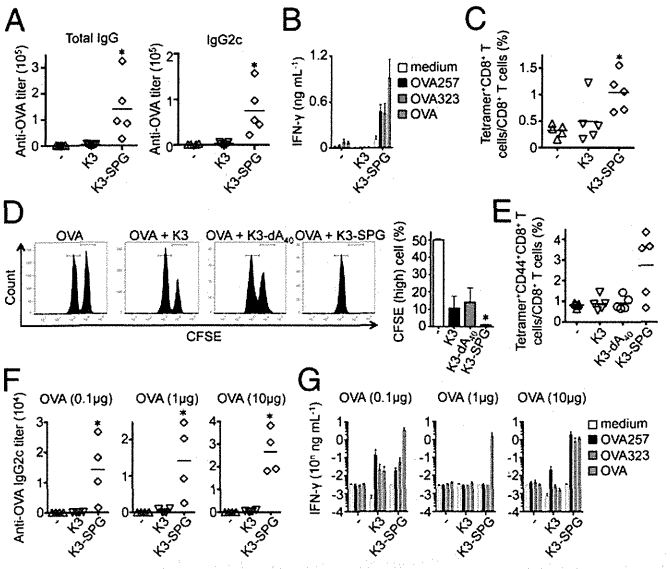

Fig. 2. K3-SPG acts as a potent vaccine adjuvant by simple mixture with antigen. Adjuvant activities of K3-SPG were analyzed. C57BL/6J mice (n = 4 or 5) were immunized s.c. with OVA protein antigen and various adjuvants. OVA-specific serum IgG (*A*), IFN-γ (*B*), and $OVA_{257–264}$-specific tetramer (*C*) were monitored (d17) after immunization (d0 and d10) with OVA (100 μg) with or without K3 (10 μg) or K3-SPG (10 μg). (*D*) In vivo CTL assay 7 d after priming with OVA and various adjuvants as indicated. (*E*) Immunization with $OVA_{257–264}$ peptide (10 μg) with or without adjuvant as indicated. (*F* and *G*) Dose-sparing study; OVA-specific serum IgG and IFN-γ were monitored after immunization as in *A* and *B*. $^*P < 0.05$ (Mann–Whitney *U* test). Data represent one of two or three independent experiments with similar results.

coadministered protein antigens lacking any covalent conjugation (Fig. 2*D*). This strong CTL induction by K3-SPG was reproduced by peptide vaccination (Fig. 2*E*) and was dose-dependent (Fig. S3). The antigen-sparing ability of K3-SPG was so potent that comparable antibody and CD4 T-cell responses were achieved using one-hundredth the amount of OVA antigen (Fig. 2 *F* and *G*). These results clearly indicate that K3-SPG is a more prominent adjuvant than K3 alone.

SPG Is a Soluble Dectin-1 Ligand but Is Not a Dectin-1 Agonist. We examined the role of Dectin-1 in cellular uptake of, and following activation by, SPG and K3-SPG, as Dectin-1 has been shown to be a receptor for β-glucans such as Zymosan (27). Using flow cytometry, we found that HEK293 cells expressing Dectin-1 but not Dectin-2 or a control (vector) increased the uptake of SPG or K3-SPG in vitro regardless of ODN presence (Fig. 3 *A* and *B*). It has recently been reported that the soluble form of β-glucan does not activate Dectin-1 signaling (28). Additionally, Dectin-1 signaling inhibits TLR9-mediated cytokine production through suppressor of cytokine signaling 1 induction (29). Therefore, we examined the agonistic activity of SPG. When splenocytes were stimulated with Zymosan-Depleted but not SPG, dose- and Dectin-1–dependent TNF-α and other cytokine production was observed, whereas cytokine production by Zymosan and Curdlan was Dectin-1–independent (Fig. 3*C* and Fig. S4). Zymosan-Depleted inhibited CpG ODN-induced IFN-α, with this inhibition relieved by Dectin-1 deficiency (Fig. 3*D*). In contrast, SPG did not inhibit CpG ODN-induced IFN-α production (Fig. 3*E*). These results indicate that SPG is a ligand but not an agonist of Dectin-1; therefore, SPG does not interfere with TLR9-mediated IFN-α production.

Adjuvant Effects of K3-SPG Are Dependent on TLR9 and Partially Dependent on Dectin-1. Because K3-SPG is a complex of CpG ODN and β-glucan, we examined the role of TLR9 (1) and Dectin-1 (30) using receptor knockout mice. When splenocytes and Flt3 ligand-induced bone marrow-derived DCs (FL-DCs) from *Tlr9*- and *Dectin-1*–deficient mice were stimulated with K3-SPG, cytokine production was completely dependent on TLR9 but not Dectin-1, excluding IL-12 p40 production (Fig. 4 *A–D*). K3-SPG–induced IL-12 p40 production showed two peaks, where the first peak of its production, but not the second peak at a higher dose, was dependent on Dectin-1 (Fig. 4*D*). This result may imply that Dectin-1 expression is involved in IL-12 p40 production at a lower dose of K3-SPG in vitro. Consistent with in vitro results, immunization of *Tlr9*-deficient mice with K3-SPG plus OVA resulted in diminished humoral and T-cell responses (Fig. 4 *E–G*). *Dectin-1*–deficient mice showed comparable immune responses with wild-type mice when the mice were immunized with OVA plus 10 μg of K3-SPG (Fig. S5). When *Dectin-1*–deficient mice were immunized with OVA plus 1 μg of K3-SPG, mice exhibited a reduced CD8 T-cell response according to the tetramer assays (Fig. 4*J*), with no significant changes in antibody and cytokine production from T cells (Fig. 4 *H* and *I*). These results suggest that the adjuvant effect of K3-SPG is dependent on TLR9 signaling. Although SPG and K3-SPG do not stimulate Dectin-1 signaling, the effect of K3-SPG is still partially dependent on Dectin-1 in vivo.

MARCO⁺, but Not Siglec-1⁺, Macrophages in Draining Lymph Nodes Dominantly Capture K3-SPG with Antigen. Given that K3-SPG provides potent adjuvant effects in vivo through immunization with a simple antigen mixture, we hypothesized that cells that capture both antigen and K3-SPG should play a critical role in mediating adjuvant effects. To examine in vivo distribution of fluorescence-labeled OVA and K3-SPG, we used fluorescence microscopy and two-photon microscopy. After an injection at the

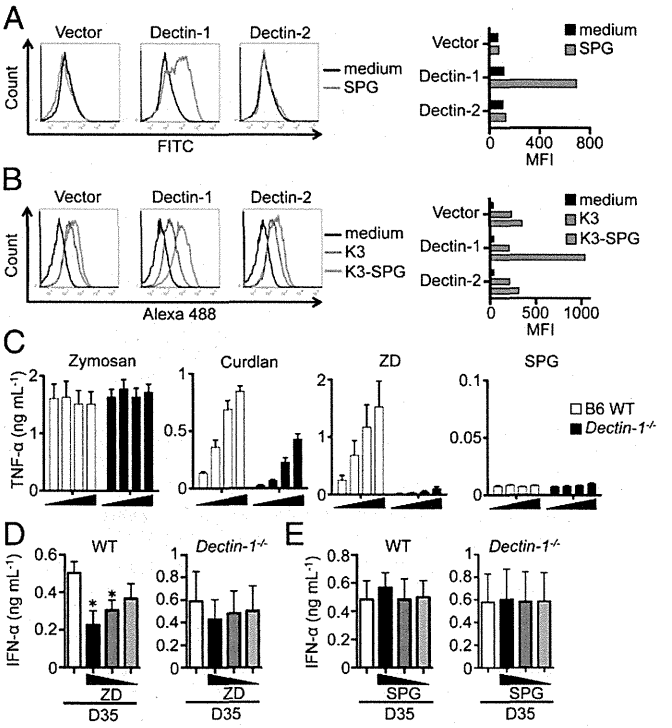

Fig. 3. SPG is a nonagonistic Dectin-1 ligand, but does not interfere with TLR9-mediated IFN-α production. (*A* and *B*) HEK293 cells transiently expressing Dectin-1 or Dectin-2 were treated with SPG-FITC (*A*), Alexa 488-K3, or Alexa 488-K3-SPG (*B*) for 60 min, and then their cellular uptake was monitored by flow cytometry [*Left*, histogram; *Right*, mean fluorescent intensity (MFI)]. Splenocytes from C57BL/6J and *Dectin-1*$^{-/-}$ mice (n = 3) were stimulated with Zymosan, Curdlan, Zymosan-Depleted (ZD), or SPG (3.7–100 μg/mL) (C), with D35 (1 μM), or with or without ZD (11.1–100 μg/mL) (*D*) or SPG (*E*) for 24 h and supernatant cytokines were monitored by ELISA. $^*P < 0.05$ (*t* test). Data represent one of three independent experiments with similar results.

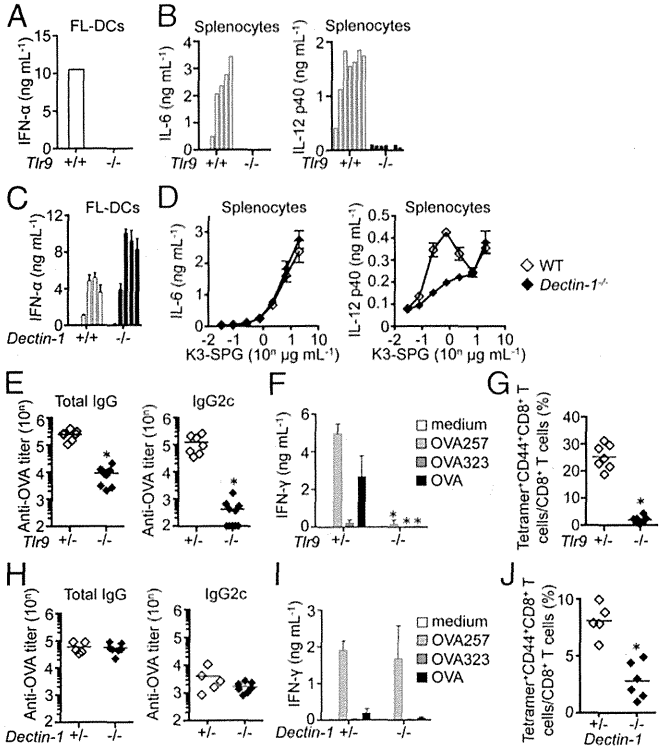

Fig. 4. Adjuvant effects of K3-SPG were completely dependent on TLR9 and partially on Dectin-1. FL-DCs (*A* and *C*) or splenocytes (*B* and *D*) from C57BL/6J, *Tlr9*$^{-/-}$, or *Dectin-1*$^{-/-}$ mice were stimulated with K3-SPG [20 μg/mL (*A*), 0.014–10 μg/mL (*B*), or 0.014–10 μg/mL (*C* and *D*)] for 24 h, and their cytokine production was monitored by ELISA. *Tlr9*$^{+/-}$ (n = 7) or *Tlr9*$^{-/-}$ mice (n = 10) (*E–G*) and *Dectin-1*$^{+/-}$ (n = 5) or *Dectin-1*$^{-/-}$ mice (n = 6) (*H–J*) were immunized s.c. with OVA (100 μg) and K3-SPG [10 μg (*E–G*) or 1 μg (*H–J*)] at days 0 and 10. Seven days after the last immunization, OVA-specific serum IgG (*E* and *H*), IFN-γ (*F* and *I*), and $OVA_{257-264}$-specific tetramer (*G* and *J*) were monitored. *$P < 0.05$ (Mann–Whitney *U* test). Data represent one of two or three independent experiments with similar results.

base of the tail, both antigen and adjuvant reached the surface of draining inguinal lymph nodes (iLNs) within 1 h (Fig. 5 *A*, *B*, and *D*). After 24 h, some K3-SPG had moved to the CD3e$^+$ T-cell area and colocalized with DQ-OVA (Fig. S6*A*). Those cells that contained both K3-SPG and DQ-OVA in the T-cell area of the iLNs were CD11c$^+$ DCs (Fig. S6*B*).

Of interest, the majority of fluorescence signals remained on the surface of the iLNs (Fig. 5*A*), prompting us to focus on two types of macrophages known to be distributed on the LN surface, Siglec-1$^+$ (also called CD169 or MOMA-1) macrophages (also known as subcapsular sinus macrophages) and MARCO$^+$ macrophages (31). Histological analysis using conventional fluorescence microscopy did not suitably reveal the entire iLN surface; moreover, these macrophages were difficult to isolate for flow cytometric analysis (32, 33). Hence, we used two-photon microscopy imaging analysis to clarify the distribution of antigen and K3-SPG ex vivo. After the injection of anti-MARCO and –Siglec-1 antibodies, specific macrophages were visualized (Movie S1). When the iLN surface was monitored by two-photon microscopy at 1 h postinjection, OVA and K3-SPG were colocalized with MARCO$^+$ but not Siglec-1$^+$ macrophages (Fig. 5 *B* and *D*, Fig. S7 *A–D*, and Movies 2–5). Previous reports suggest that the immune complex and inactivated influenza virus are captured by Siglec-1$^+$ macrophages to induce humoral immune responses (34, 35). The distribution pattern perfectly matched that for MARCO$^+$ macrophages in the iLNs and did not colocalize with Siglec-1$^+$ macrophages, as confirmed by Volocity's colocalization analysis (Perkin Elmer) (Fig. 5 *B–E*). In contrast, K3 was more diffusely distributed between MARCO$^+$ and Siglec-1$^+$ areas compared with K3-SPG (Fig. 5 *D* and *E*, Fig. S7 *C–E*, and Movies 6 and 7). Additionally, both *Tlr9*- and *Dectin-1*–deficient mice showed comparable localization of K3-SPG (Fig. S7 *F* and *G*).

To determine the contribution of these macrophages toward the adjuvant effects of K3-SPG, we examined different recovery kinetics of macrophages and DCs following an injection of clodronate liposomes into the base of the tail. After the injection, the macrophages were completely depleted by day 2. These cells did not recover for at least 1 wk, whereas DCs were mostly recovered by day 7, as previously reported (36). When both macrophages and DCs were depleted, immune responses were significantly suppressed [Fig. 5*F*, Clo (–d2)]. When only macrophages, but not DCs, were depleted, the immune responses were comparable to those in untreated mice [Fig. 5*F*, Clo (–d7)]. This would suggest that although both OVA and K3-SPG were mainly captured by

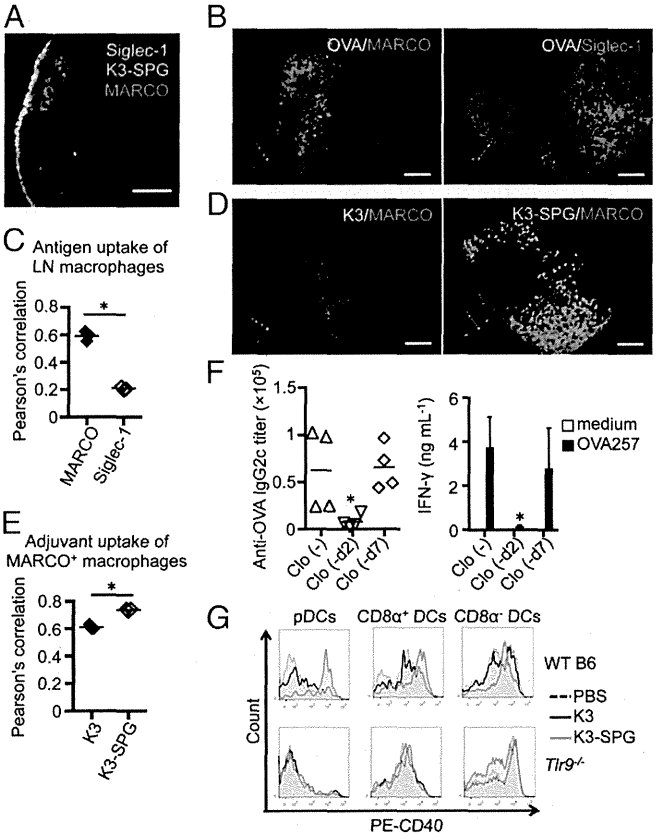

Fig. 5. Role of lymph node macrophages and dendritic cells in uptake and adjuvant effects of K3-SPG. (*A*) Immunohistochemistry of mouse inguinal LNs after Alexa 488-K3-SPG injection. One hour after injection, the LNs were collected and stained with anti–MARCO-phycoerythrin (PE) and anti–Siglec-1-APC antibodies. (*B–E*) Two-photon microscopic analysis of LNs. DQ-OVA, Alexa 488-K3, or Alexa 488-K3-SPG was injected as indicated, and anti–MARCO-PE or anti–Siglec-1-PE antibodies were administered. The LNs were collected 1 h later and analyzed by two-photon microscopy. (*C* and *E*) Colocalization of antigen or adjuvant with the stained macrophages was analyzed by Pearson's correlation. (*F*) Clodronate liposomes were injected into C57BL/6J mice either 2 or 7 d before immunization (n = 4). Mice were administered OVA (100 μg) plus K3-SPG (10 μg) at day 0. Eight days after immunization, OVA-specific serum IgG and IFN-γ were monitored. (*G*) C57BL/6J and *Tlr9*$^{-/-}$ mice were administered s.c. with K3 (10 μg) or K3-SPG (10 μg). At 24 h postadministration, the LNs were collected and the prepared cells were stained and analyzed by flow cytometry. (Scale bars, 100 μm.) *$P < 0.05$ (*t* test or Mann–Whitney *U* test). Data represent one of two or three independent experiments with similar results.

MARCO$^+$ macrophages in the LNs after injection, the macrophages were dispensable to inducing adaptive immune responses. In other words, the adjuvant effect of K3-SPG was largely dependent on the DC population.

K3-SPG Targets and Strongly Activates the Antigen-Bearing DC Population in Vivo. Our findings suggest that although a large portion of nanoparticulate K3-SPG was taken up by MARCO$^+$ macrophages in iLNs after injection, the adjuvant effects appear to be controlled by DCs. We focused on antigen and adjuvant uptake by the DC population in iLNs. At 24 h postinjection, the uptake of antigen and adjuvants by the DC population was analyzed by flow cytometry. The frequency of CpG-positives in three DC subsets (pDCs, CD8α$^+$ DCs, and CD8α$^-$ DCs) was significantly increased after K3-SPG injection than with K3 (Fig. S8*A*). In contrast, the frequency of OVA-positive DCs was comparable after K3 and K3-SPG injections (Fig. S8*B*). When we focused on both antigen- and adjuvant-positive DCs, there was a substantial increase for K3-SPG over K3 (Fig. S9). Both pDCs and CD8α$^+$ DCs in iLNs were strongly activated by K3-SPG but not by K3 24 h postinjection, and this was completely dependent on TLR9 (Fig. 5*G*). Our results indicate that pDCs and CD8α$^+$ DCs preferentially capture nanoparticulate K3-SPG rather than nonparticulate K3 for maturation and to exert adjuvant effects.

K3-SPG Is a Potent Adjuvant for Influenza Vaccine in Murine and Nonhuman Primate Models. Finally, we sought the adjuvant effect of K3-SPG by using more clinically relevant influenza vaccination models in both mice and nonhuman primates. When mice were immunized with ether-treated hemagglutinin antigen-enriched virion-free split vaccine (SV) plus the indicated adjuvant, K3-SPG demonstrated superior adjuvant effects to K3 when antibody responses (Fig. S10*A*) and T-cell responses (Fig. S10*B*) were compared. More importantly, SV plus K3-SPG immunization resulted in a 100-fold greater antibody response, even compared with vaccination using a whole (virion) inactivated vaccine (WIV) (0.2 μg per mouse) (Fig. 6*A*), which contains viral RNA as a built-in adjuvant (21). Interestingly, SV (0.1 μg per mouse) plus K3-SPG strongly induced both CD8 and CD4 T-cell responses (Fig. 6*B*). Mice immunized with SV and K3-SPG exhibited less body weight loss than WIV-immunized mice (Fig. 6*C*). Strikingly, K3-SPG conferred 100% protection against lethal PR8 virus challenge at the dose of which only 10% of WIV-vaccinated mice survived (Fig. 6*D*). These results strongly support the notion that K3-SPG works as a potent adjuvant for protein or protein-based vaccines in a murine model, prompting us to extend this finding to a nonhuman primate model using the cynomolgus monkey (*Macaca fascicularis*). Each group of three cynomolgus monkeys was immunized with SV plus K3 or K3-SPG at days 0 and 14. Serum antibody titers were then monitored for 8 wk. The SV plus K3-SPG induced significantly higher antibody titer at 2 wk postimmunization, and titer levels remained high for at least another 6 wk (Fig. 6*E*). Although antibody titers were reduced at 110 wk after immunization, the K3-SPG group had higher antibody titers than the K3 group (Fig. 6*E*). When PBMCs were stimulated with SV and WIV, IFN-γ was detected from the SV plus K3-SPG–immunized group (Fig. 6*F*). Taken together, these results suggest that K3-SPG is a prominent vaccine adjuvant in a nonhuman primate model.

Discussion

The medical need for novel, potent, and safe adjuvants is ever-increasing these days as (*i*) recombinant vaccine antigens such proteins and peptides are short on natural adjuvants, unlike attenuated or inactivated whole microbial antigens, (*ii*) conventional aluminum salts and oil adjuvants are limited or preferred for enhancing humoral immune responses, and (*iii*) new adjuvants that can induce cellular immune responses, including CTLs, are needed, for example for cancer vaccines. The last two decades have resulted in tremendous progress with respect to adjuvant research and development. A hallmark of the new generation of adjuvants is that nucleic acids have been rediscovered to be immunologically active in stimulating specific innate immune receptors of the host, in particular TLRs. CpG DNA, a ligand for TLR9, is one of the most promising immunotherapeutic agents that has been identified.

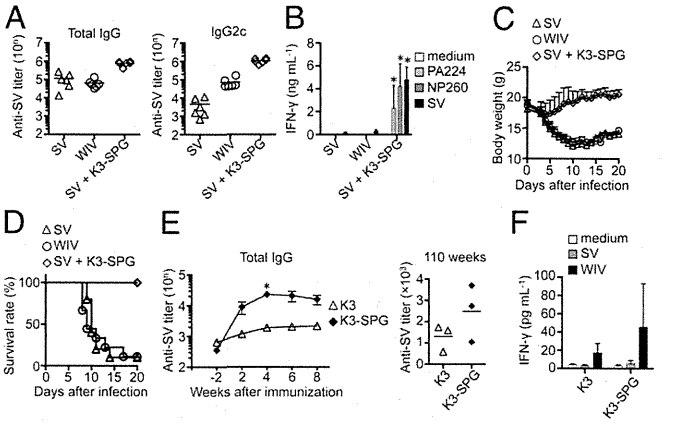

Fig. 6. K3-SPG acts as an influenza vaccine adjuvant in mice and nonhuman primates. (*A–D*) C57BL/6J mice (n = 6 or 10) were immunized with SV (0.1 μg), whole inactivated vaccine (WIV) (0.2 μg), or SV (0.1 μg) plus K3-SPG (10 μg) at days 0 and 14. Seven days after the final immunization, SV-specific serum IgG titers (*A*) and IFN-γ (*B*) [specific to SV antigen, $PA_{224–233}$ (PA224) (10 μg/mL) or $NP_{260–283}$ (NP260)] were monitored. (*C* and *D*) Fourteen days after the final immunization, mice were challenged with a 10-LD_{50} dose of influenza virus A/PR/8 (H1N1). Changes in body weights (*C*) and mortality (*D*) were monitored for the next 20 d. (*E* and *F*) Cynomolgus monkeys (n = 3) were immunized with SV (5 μg) plus K3 (5 nmol) or SV plus K3-SPG (5 nmol) at days 0 and 14. (*E*) Serum samples were collected at −2, 2, 4, 6, 8, and 110 wk. Antigen-specific serum antibody titers were measured by ELISA. (*F*) PBMCs were prepared from individual cynomolgus monkey blood at 4 wk after the first immunization and restimulated in vitro with medium, SV (10 μg), or WIV for 24 h. Mouse IFN-γ in the supernatants was determined by ELISA. *P < 0.05 (t test or Mann–Whitney U test).

Although there are several types of potent humanized CpG ODN—K (also called B), D (A), C, and P types—the development of an all-in-one CpG ODN activating both B cells and pDCs to form a stable nanoparticle without aggregation has been less than successful. In this study, we generated a novel K CpG ODN that we designated K3-SPG. Although it had been reported that there are molecular interactions between single-stranded nucleic acids and β-glucan (37) and that murine and humanized CpG ODNs can be wrapped by SPG to increase their original TLR9-agonistic activities (20), our report demonstrates that a rod-shaped nano-sized K3-SPG particle exhibits dual characteristics of K and D CpG ODNs (Fig. 1). K3-SPG is distinct from other previously reported K CpG ODNs, including K3. In turn, K3-SPG becomes a D CpG ODN, stimulating human PBMCs to produce large amounts of both type I and type II IFN, targeting the same endosome where the IFN-inducing D type resides without losing its K-type activity (Fig. 1 *F* and *G*). Another surprising finding is that this K3-SPG forms a rod-like single nanomolecule (Fig. 1 *C* and *D*). This is advantageous over previously demonstrated D or P types, whose ends form higher-order structures that may hamper further development as prodrugs, including good manufacturing practice assignment.

Another prominent feature of this K3-SPG is its potency as an adjuvant for induction of both humoral and cellular immune responses, especially CTL induction, to coadministered protein antigens without conjugation. Such potent adjuvant activity of K3-SPG is attributable to its nanoparticulate nature (Figs. 1 *C* and *D* and 2) rather than targeting Dectin-1 by SPG (Figs. 3 and 4). Initially, we hypothesized that K3-SPG becomes such a potent adjuvant because it targets Dectin-1, because SPG is a β-1,3-glucan, and seems to be a clear Dectin-1 ligand (Fig. 3*A*). Our other results, however, led us to conclude that the role of Dectin-1

in vivo with respect to the adjuvant activity of K3-SPG was minimal (Fig. 4). More importantly, the in vivo activity of K3-SPG was completely dependent upon TLR9 (Fig. 4 *E–G*). SPG is a soluble Dectin-1 ligand but not a Dectin-1 agonist, and thus does not interfere with TLR9-mediated DC activation (Fig. 3 *D* and *E*). The adjuvant activity of K3-SPG is mostly independent of Dectin-1, except at very low doses during the immunization protocol (Fig. 4*J*). Instead, some other receptors such as C-type lectins, Siglecs, and scavenger receptors may play roles in delivering SPG into macrophages and/or DCs, accumulating and activating antigen-bearing macrophages and DCs in draining lymph nodes (Fig. 5). In this regard, we also found that $MARCO^+$, but not Siglec-1^+, macrophages in draining lymph nodes are dominant in capturing K3-SPG, and coadministered antigen (LPS-free OVA protein), and that K3-SPG targets the antigen-bearing DC population in vivo. Although the depletion of macrophages did not ameliorate adjuvant effects, large amounts of antigen and K3-SPG are taken up by the same $MARCO^+$ macrophages, and the two-photon microscopic data suggest that they are activated as they become much bigger than nonstimulated macrophages. Whether this massive accumulation of antigen and adjuvant in $MARCO^+$ macrophages contributes to the following DC activation and adaptive T- and B-cell activation is yet to be elucidated in future work.

The protective potency of K3-SPG as an influenza vaccine adjuvant was demonstrated in vivo in both murine and nonhuman primate models. In the murine model, intradermal immunization with a very low dose of seasonal influenza split vaccine mixed with K3-SPG in solution provoked robust IgG responses and offered better protection than a low but physiological dose of whole inactivated virion vaccination against the heterologous challenge of lethal virus (Fig. 6 *C* and *D*). These data provide better protective potency than our previous results, where we used approximately 10 times higher doses of influenza antigens (21), because many factors for K3-SPG have been improved for its potency: K3–SPG complexation efficiency and optimization of the order between K3 and poly(dA_{40}) (Fig. 1); the immunization route is different as well. The data above prompted us to develop K3-SPG as a potent adjuvant for influenza split vaccine, especially for those urgently needing improvement: seasonal influenza vaccination for the elderly, immunodeficient patients (transplant recipients), and pandemic influenza vaccination.

Taken together, these data suggest that K3-SPG can be used as a potent adjuvant for protein vaccines such as influenza split vaccines, and may be useful for immunotherapeutic applications that require type I and type II IFN as well as CTL induction.

Materials and Methods

All animal studies using mice and monkeys were conducted in accordance with the Institutional Animal Care and Use Committee at the National Institute of Biomedical Innovation. All of the ODNs used in this manuscript were synthesized by GeneDesign. Other details are described in *SI Materials and Methods*.

ACKNOWLEDGMENTS. This study was supported by a Health and Labour Sciences Research Grant and the Japan Science and Technology Agency Core Research for Evolutionary Science and Technology Program.

1. Hemmi H, et al. (2000) A Toll-like receptor recognizes bacterial DNA. *Nature* 408(6813):740–745.
2. Krieg AM (2006) Therapeutic potential of Toll-like receptor 9 activation. *Nat Rev Drug Discov* 5(6):471–484.
3. Chu RS, Targoni OS, Krieg AM, Lehmann PV, Harding CV (1997) CpG oligodeoxynucleotides act as adjuvants that switch on T helper 1 (Th1) immunity. *J Exp Med* 186(10):1623–1631.
4. Brazolot Millan CL, Weeratna R, Krieg AM, Siegrist CA, Davis HL (1998) CpG DNA can induce strong Th1 humoral and cell-mediated immune responses against hepatitis B surface antigen in young mice. *Proc Natl Acad Sci USA* 95(26):15553–15558.
5. Klinman DM (2004) Immunotherapeutic uses of CpG oligodeoxynucleotides. *Nat Rev Immunol* 4(4):249–258.
6. Vollmer J, Krieg AM (2009) Immunotherapeutic applications of CpG oligodeoxynucleotide TLR9 agonists. *Adv Drug Deliv Rev* 61(3):195–204.
7. Krug A, et al. (2001) Identification of CpG oligonucleotide sequences with high induction of IFN-alpha/beta in plasmacytoid dendritic cells. *Eur J Immunol* 31(7): 2154–2163.
8. Verthelyi D, Ishii KJ, Gursel M, Takeshita F, Klinman DM (2001) Human peripheral blood cells differentially recognize and respond to two distinct CpG motifs. *J Immunol* 166(4):2372–2377.
9. Hartmann G, Krieg AM (2000) Mechanism and function of a newly identified CpG DNA motif in human primary B cells. *J Immunol* 164(2):944–953.
10. Hartmann G, et al. (2003) Rational design of new CpG oligonucleotides that combine B cell activation with high IFN-alpha induction in plasmacytoid dendritic cells. *Eur J Immunol* 33(6):1633–1641.
11. Marshall JD, et al. (2003) Identification of a novel CpG DNA class and motif that optimally stimulate B cell and plasmacytoid dendritic cell functions. *J Leukoc Biol* 73(6):781–792.
12. Samulowitz U, et al. (2010) A novel class of immune-stimulatory CpG oligodeoxynucleotides unifies high potency in type I interferon induction with preferred structural properties. *Oligonucleotides* 20(2):93–101.
13. Kerkmann M, et al. (2005) Spontaneous formation of nucleic acid-based nanoparticles is responsible for high interferon-alpha induction by CpG-A in plasmacytoid dendritic cells. *J Biol Chem* 280(9):8086–8093.
14. Klein DC, Latz E, Espevik T, Stokke BT (2010) Higher order structure of short immunostimulatory oligonucleotides studied by atomic force microscopy. *Ultramicroscopy* 110(6):689–693.
15. Puig M, et al. (2006) Use of thermolytic protective groups to prevent G-tetrad formation in CpG ODN type D: Structural studies and immunomodulatory activity in primates. *Nucleic Acids Res* 34(22):6488–6495.
16. McHutchison JG, et al. (2007) Phase 1B, randomized, double-blind, dose-escalation trial of CPG 10101 in patients with chronic hepatitis C virus. *Hepatology* 46(5): 1341–1349.
17. Bode C, Zhao G, Steinhagen F, Kinjo T, Klinman DM (2011) CpG DNA as a vaccine adjuvant. *Expert Rev Vaccines* 10(4):499–511.
18. Okamura K, et al. (1986) Clinical evaluation of schizophyllan combined with irradiation in patients with cervical cancer. A randomized controlled study. *Cancer* 58(4): 865–872.
19. Sakurai K, Mizu M, Shinkai S (2001) Polysaccharide—polynucleotide complexes. 2. Complementary polynucleotide mimic behavior of the natural polysaccharide schizophyllan in the macromolecular complex with single-stranded RNA and DNA. *Biomacromolecules* 2(3):641–650.
20. Shimada N, et al. (2007) A polysaccharide carrier to effectively deliver native phosphodiester CpG DNA to antigen-presenting cells. *Bioconjug Chem* 18(4):1280–1286.
21. Koyama S, et al. (2010) Plasmacytoid dendritic cells delineate immunogenicity of influenza vaccine subtypes. *Sci Transl Med* 2(25):25ra24.
22. Minari J, et al. (2011) Enhanced cytokine secretion from primary macrophages due to Dectin-1 mediated uptake of CpG DNA/β-1,3-glucan complex. *Bioconjug Chem* 22(1):9–15.
23. Bae AH, et al. (2004) Rod-like architecture and helicity of the poly(C)/schizophyllan complex observed by AFM and SEM. *Carbohydr Res* 339(2):251–258.
24. Costa LT, et al. (2004) Structural studies of oligonucleotides containing G-quadruplex motifs using AFM. *Biochem Biophys Res Commun* 313(4):1065–1072.
25. Gürsel M, Verthelyi D, Gürsel I, Ishii KJ, Klinman DM (2002) Differential and competitive activation of human immune cells by distinct classes of CpG oligodeoxynucleotide. *J Leukoc Biol* 71(5):813–820.
26. Guiducci C, et al. (2006) Properties regulating the nature of the plasmacytoid dendritic cell response to Toll-like receptor 9 activation. *J Exp Med* 203(8):1999–2008.
27. Herre J, et al. (2004) Dectin-1 uses novel mechanisms for yeast phagocytosis in macrophages. *Blood* 104(13):4038–4045.
28. Goodridge HS, et al. (2011) Activation of the innate immune receptor Dectin-1 upon formation of a 'phagocytic synapse.' *Nature* 472(7344):471–475.
29. Eberle ME, Dalpke AH (2012) Dectin-1 stimulation induces suppressor of cytokine signaling 1, thereby modulating TLR signaling and T cell responses. *J Immunol* 188(11):5644–5654.
30. Saijo S, et al. (2007) Dectin-1 is required for host defense against *Pneumocystis carinii* but not against *Candida albicans*. *Nat Immunol* 8(1):39–46.
31. Martinez-Pomares L, Gordon S (2012) $CD169^+$ macrophages at the crossroads of antigen presentation. *Trends Immunol* 33(2):66–70.
32. Aoshi T, et al. (2009) The cellular niche of *Listeria monocytogenes* infection changes rapidly in the spleen. *Eur J Immunol* 39(2):417–425.
33. Gray EE, Cyster JG (2012) Lymph node macrophages. *J Innate Immun* 4(5-6):424–436.
34. Suzuki K, Grigorova I, Phan TG, Kelly LM, Cyster JG (2009) Visualizing B cell capture of cognate antigen from follicular dendritic cells. *J Exp Med* 206(7):1485–1493.
35. Gonzalez SF, et al. (2010) Capture of influenza by medullary dendritic cells via SIGN-R1 is essential for humoral immunity in draining lymph nodes. *Nat Immunol* 11(5): 427–434.
36. Aoshi T, et al. (2008) Bacterial entry to the splenic white pulp initiates antigen presentation to $CD8^+$ T cells. *Immunity* 29(3):476–486.
37. Sakurai K, Shinkai S (2000) Phase separation in the mixture of schizophyllan and poly (ethylene oxide) in aqueous solution driven by a specific interaction between the glucose side chain and poly(ethylene oxide). *Carbohydr Res* 324(2):136–140.

OPEN ACCESS Freely available online

PLOS ONE

Effects of Mycobacteria Major Secretion Protein, Ag85B, on Allergic Inflammation in the Lung

Yusuke Tsujimura[1], Hiroyasu Inada[2], Misao Yoneda[3], Tomoyuki Fujita[4], Kazuhiro Matsuo[5], Yasuhiro Yasutomi[1,6]*

1 Laboratory of Immunoregulation and Vaccine Research, Tsukuba Primate Research Center, National Institute of Biomedical Innovation, Tsukuba, Ibaraki, Japan, **2** Department of Pharmaceutical Sciences, Suzuka University of Medical Science, Suzuka, Mie, Japan, **3** Department of Pathologic Oncology, Institute of Molecular and Experimental Medicine, Faculty of Medicine, Mie University Graduate School of Medicine, Tsu, Mie, Japan, **4** Research Laboratories, Kyoto R&D Center, Maruho Co., Ltd, Chudoji, Shimogyo-ku, Kyoto, Japan, **5** Research and Development Department, Japan BCG Laboratory, Kiyose, Tokyo, Japan, **6** Department of Immunoregulation, Mie University Graduate School of Medicine, Tsu, Mie, Japan

Abstract

Many epidemiological studies have suggested that the recent increase in prevalence and severity of allergic diseases such as asthma is inversely correlated with *Mycobacterium bovis* bacillus Calmette Guerin (BCG) vaccination. However, the underlying mechanisms by which mycobacterial components suppress allergic diseases are not yet fully understood. Here we showed the inhibitory mechanisms for development of allergic airway inflammation by using highly purified recombinant Ag85B (rAg85B), which is one of the major protein antigens secreted from *M. tuberculosis*. Ag85B is thought to be a single immunogenic protein that can elicit a strong Th1-type immune response in hosts infected with mycobacteria, including individuals vaccinated with BCG. Administration of rAg85B showed a strong inhibitory effect on the development of allergic airway inflammation with induction of Th1-response and IL-17and IL-22 production. Both cytokines induced by rAg85B were involved in the induction of Th17-related cytokine-production innate immune cells in the lung. Administration of neutralizing antibodies to IL-17 or IL-22 in rAg85B-treated mice revealed that IL-17 induced the infiltration of neutrophils in BAL fluid and that allergen-induced bronchial eosinophilia was inhibited by IL-22. Furthermore, enhancement of the expression of genes associated with tissue homeostasis and wound healing was observed in bronchial tissues after rAg85B administration in a Th17-related cytokine dependent manner. The results of this study provide evidence for the potential usefulness of rAg85B as a novel approach for anti-allergic effect and tissue repair other than the role as a conventional TB vaccine.

Citation: Tsujimura Y, Inada H, Yoneda M, Fujita T, Matsuo K, et al. (2014) Effects of Mycobacteria Major Secretion Protein, Ag85B, on Allergic Inflammation in the Lung. PLoS ONE 9(9): e106807. doi:10.1371/journal.pone.0106807

Editor: Yoshihiko Hoshino, National Institute of Infectious Diseases, Japan

Received April 18, 2014; **Accepted** August 6, 2014; **Published** September 5, 2014

Data Availability: The authors confirm that all data underlying the findings are fully available without restriction. All relevant data are within the paper and its Supporting Information files.

Funding: This work was supported by Health Science Research Grants from the Ministry of Health, Labor, and Welfare of Japan and the Ministry of Education, Culture, Sports, Science, and Technology of Japan. The funders had no role in study design, data collection and analysis, decision to publish, or preparation of the manuscript.

Competing Interests: The authors have no commercial or financial conflict of interest. The authors also have no competing interest in Maruho Co., Ltd. This does not alter the authors' adherence to PLOS ONE policies on sharing data and materials.

* Email: yasutomi@nibio.go.jp

Introduction

Epidemiological studies showed that treatments with bacterial and viral products might be effective therapeutic strategies for suppressing the development of allergic responses [1–3]. Administration of mycobacteria, including *Mycobacterium bovis*-Bacillus Calmette Guerin (BCG), has been thought to be effective for preventing the development of asthma by induction of Th1-type immune responses [4], regulatory T (Treg) cells [5,6] and NKT cells [7,8]. On the other hand, recent data have revealed that *Mycobacterium tuberculosis* infection induced not only IFN-γ but also IL-17, which promotes granuloma organization followed by neutrophil recruitment, and IL-22, which promotes regeneration and protects against tissue damage [9]. In addition, vaccination with the mycobacteria-secreted immunogenic protein Ag85A had important links with Th1/Th17 cell induction and Treg cell reduction [10]. However, the role of mycobacteria-mediated Th17-related cytokines in allergic asthma remains unknown.

The airway epithelium and innate immune cells are considered to be essential controllers of inflammatory, immune and regenerative responses to allergens that contribute to asthma pathogenesis [11]. Dysfunction of the epithelium leading to chronic injury was suggested to be a consequence of sustained airway inflammation that is associated with Th2-driven adaptive immunity [12]. Tissue homeostasis at exposed surfaces of the lung is regulated by Th17-related cytokines, especially IL-22, in the innate immune system [13]. Therefore, the functional and structural maintenance of tissue might be necessary to induce both innate and adaptive immunity.

One immunogenic protein that can induce a strong Th1-type immune response in hosts sensitized by BCG is thought to be Ag85B. Ag85B is one of the most dominant protein antigens secreted from all mycobacterial species and has been shown to

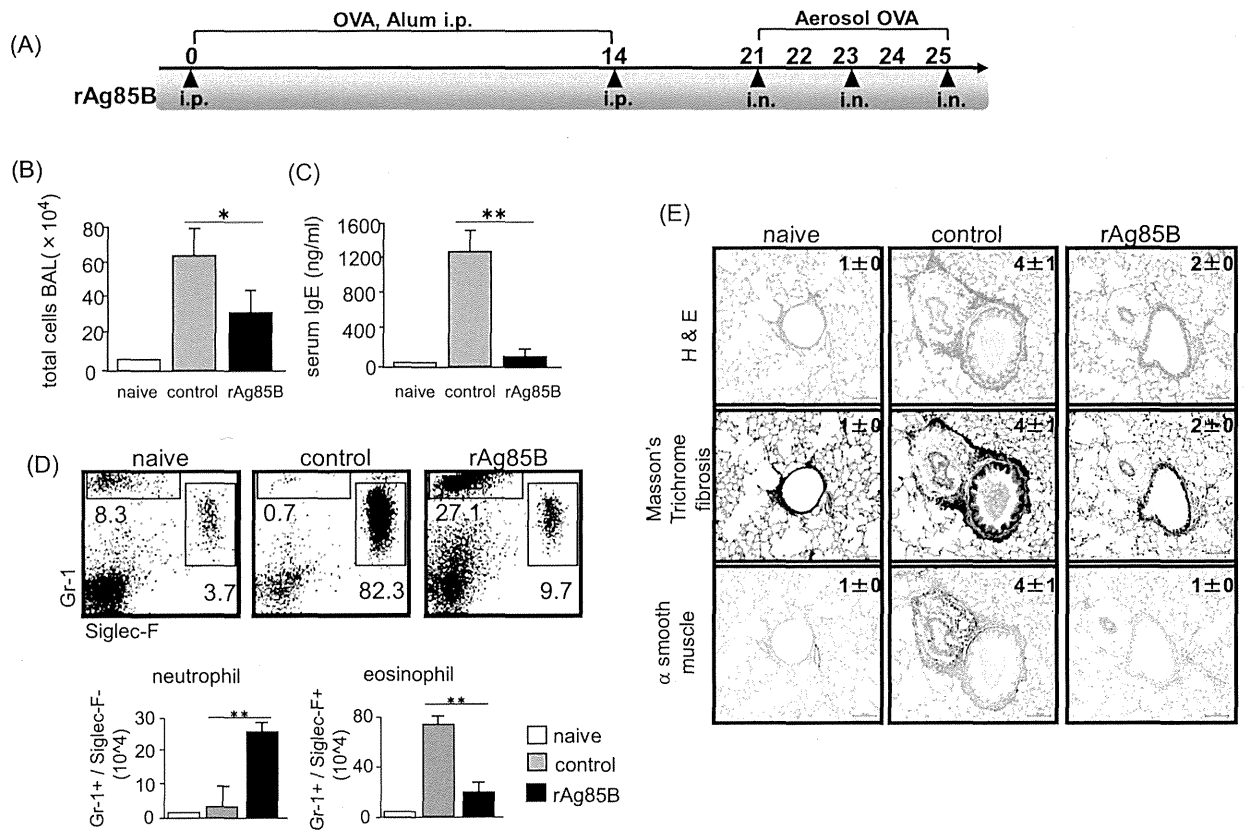

Figure 1. Functions of rAg85B in allergic inflammation. Experimental design used to investigate the effects of rAg85B on OVA-induced allergic lung inflammation (*A*). BALB/c mice were intraperitoneally immunized with OVA on days 0 and 14. On days 21 to 25 after the first immunization, mice were exposed to aerosolized 5% OVA for 20 min. Three hours prior to OVA inhalation, the mice were i.p. (100 μg; days 0 and 14) and i.n. (20 μg; days 21, 23, and 25) administered rAg85B. One day after the last challenge, the BAL cells were counted (*B*) and OVA-specific serum IgE concentrations were determined by ELISA (*C*). Flow cytometry of BAL cells from naïve or OVA sensitized BALB/c mice treated with PBS or rAg85B, stained with anti-Gr-1 and anti-Siglec-F. Numbers adjacent to outlined area indicate percent of eosinophils (Gr-1^{dull}, Siglec-F^{+}), and neutrophils (Gr-1^{+}, Siglec-F^{neg}) (*D*). Formalin-fixed tissue sections were stained with hematoxylin and eosin to visualized cell recruitment (upper row, scale bar, 100 mm), Masson's trichrome (center row, scale bar, 100 mm), and α-smooth muscle actin (lower row, scale bar, 50 mm). Numbers in quadrants indicate the score scale from 0 to 5 in each. (*E*). Data are representative of at least three independent experiments. (*P<0.05, **P<0.01 compared with OVA control. error bars, s.d.; *n* = 6 mice).
doi:10.1371/journal.pone.0106807.g001

induce substantial Th cell proliferation and vigorous Th1 cytokine production in humans and mice [14]. In addition, we have reported the possibility of using Ag85B DNA as an immunological strategic tool to induce both Th1 and Treg cells in immunotherapy for atopic dermatitis and allergic asthma [15,16].

In the present study, we found that highly purified recombinant Ag85B protein (rAg85B) had suppressive effects depending on induction of Th1 immune responses in a mouse model of allergic lung inflammation. Remarkably, rAg85B administration also promoted IL-17 and IL-22 production in both Th17 cells in lymph nodes (LNs) and various innate immune cells such as gamma delta T (γδT) cells, NKp46^{+} cells, lymphoid tissue inducer (LTi)-like cells, and CD11c^{+} cells in BAL fluid. More interestingly, Th17-related cytokines induced by rAg85B were involved in enhancement of the expression of genes related to maintenance of tissue homeostasis. This is the first report demonstrating that mycobacteria major secreting protein Ag85B plays an important role in the regulation of allergic airway inflammation by inducing not only a Th1-response but also recruitment of an IL-17 and/or IL-22-producing Th cell subset in LNs and innate immune BAL cells in a manner dependent on Th17-related cytokines in order to retain tissue integrity.

Materials and Methods

Animal and Ethic Statement

Specific pathogen-free BALB/c mice (six-week-old, female) were purchased from CLEA Japan. All of the experiments in this study were performed in accordance with the Guidelines for Animal Use and Experimentation, as set out by the National Institute of Biomedical Innovation. The protocol was approved by the Animal Welfare and Animal Care Committee of the National Institute of Biomedical Innovation (Permit Number: DS23-8R2). All animal procedures were used to minimize animal pain and suffering.

Experimental protocol

BALB/c mice were intraperitoneally immunized with 10 μg ovalbumin (OVA) with 1 mg aluminum hydroxide on days 0 and 14. On days 21 to 25 after the first immunization, mice were exposed to aerosolized 5% OVA for 20 min. Three hours prior to

OVA inhalation, the mice were intraperitoneally (i.p.) (100 μg; days 0 and 14) and intranasal ly (i.n.) (20 μg; days 21, 23, and 25) administered rAg85B. OVA-sensitized Balb/c mice were challenged intranasally with PBS, rAg85B, rAg85B plus 5 μg anti-IL-17 Abs and/or 10 μg anti-IL-22 Abs (R&D Systems) with the same time course as that of rAg85B i.n. administration. The isotype-matched control antibody for neutralization experiments was set using normal goat IgG control (R&D systems).

Recombinant protein Ag85B production

Plasmids containing the Ag85B gene were transformed into *E. coli* TG1. The expressed inclusion body (IB) was harvested from the disrupted cell pellet by a homogenizer with lysis buffer (30 mM sodium phosphaste, 100 mM NaCl, 5 mM EDTA and 0.5% Triton X-100). This IB of Ag85B was unfolded in 8 M urea and refolded by dilution to 0.4 M urea. The urea in the refolding buffer was removed by anion exchange chromatography using 20 mM Tris buffer and 20 mM Tris buffer with 1 M NaCl (pH 8.5). The refolded Ag85B was loaded on a cation exchange column, and crude Ag85B was passed through the resin using 50 mM NaOAc buffer and 50 mM NaOAc buffer with 1 M NaCl (pH 6.0). Finally, Ag85B was purified by anion exchange chromatography using 20 mM Tris buffer and 20 mM Tris buffer with 1 M NaCl (pH 7.6).

Endotoxin test

The endotoxin value of Ag85B was measured by Kinetic turbidimetric LAL assay kit (Lonza). Test was carried out according to the manufacture's instruction. The endotoxin value was measured kinetically on ELISA after mixing sample and LAL reagent and was calculated automatically according to standard curve. Purified Ag85B had a purity of >95% analyzed by SDS-PAGE and contaminated less than 0.02 EU/mg of endotoxin. Protein quantitation was carried out by UV spectroscopy at 280 nm.

Isolation and analysis of lymph node and BAL cells

BAL cells were prepared according to a published protocol [16]. Single cell suspensions from BAL fluid and mediastinal lymph nodes (MLNs) were obtained by crushing through cell strainers. Cells were stained with antibodies to the following markers: CD3, CD4, CD8, CD19, CD11b, CD11c, CD25, γδ TCR, NKp46, Gr-1, Siglec-F, CD127, IFN-γ, IL-4, Foxp3, IL-17 and IL-22 (BD). For analysis of intracellular cytokine production, cells were stimulated directly by incubation for 5 h with 50 ng/ml PMA and 750 ng/ml ionomycin (Sigma-Aldrich) at 37°C and with 10 μg/ml brefeldin A (eBioscience) added in the last 3 h. Flow cytometry data collection was performed on a FACS Calibur (BD). Files were analyzed using CellQuest Software (BD).

Quantification of cytokines and chemokines

Concentrations of cytokines and chemokines in BAL fluid and culture supernatants of OVA-restimulated lymph node cells were determined by ELISA using commercial kits from R&D Systems. Twenty-four hours after the last OVA sensitization, MLNs and BAL fluid were harvested. MLNs were cultured with 50 μg/ml OVA, and cytokines in the culture supernatant were determined 48 h after incubation. The BAL fluid were measured directly.

Lung histology

The organs were removed and placed in 4% buffered paraformaldehyde (PFA) overnight. Excess paraformaldehyde was removed by incubation in fresh PBS. Fixed tissues were incubated at 4°C in 70% ethanol. PFA-fixed lung sections were stained with hematoxylin and eosin, Masson's trichrome, and α-smooth muscle actin. Peribronchial infiltrates, fibrosis, and smooth muscle hyperplasia were assessed by a semiquantitative score (0–5) by a pathologist.

Quantitative real-time PCR

RNA was isolated from whole lung tissue using mechanical homogenization and TRIzol reagent (Invitrogen) according to the manufacturer's instructions. RNA concentrations were measured with a Nanodrop ND 1000 (Nucliber). Omniscript reverse tanscriptase was used according to the protocol of the manufacturer (QIAGEN) for the production of cDNA in a reaction volume of 20 ul. Primers for quantitative real-time RT-PCR were designed with the Universal ProbeLibrary Assay Design Center (Roche Applied Science). Reactions were run on an RT-PCR system (LightCycler 480; Roche Applied Science) Samples were normalized to b-actin and displayed as fold induction over naïve or untreated controls unless otherwise stated.

TLR/NLR ligand screening

The presence of TLR and NLR ligands were tested on recombinant human embryonic kidney 293 (HEK293) cell lines

Table 1. Effects of rAg85B to Toll-Like and NOD-Like Receptor.

receptor	No ligand	rAg85B	control (+)
mTLR2	0.1±0.0	0.1±0.0	2.3±0.1
mTLR3	0.1±0.0	0.1±0.0	2.4±0.2
mTLR4	0.1±0.0	0.1±0.0	2.7±0.1
mTLR5	0.1±0.0	0.1±0.0	2.7±0.1
mTLR7	0.1±0.0	0.1±0.0	2.1±0.0
mTLR8	0.1±0.0	0.1±0.0	2.3±0.1
mTLR9	0.1±0.0	0.1±0.0	2.6±0.1
mNOD1	0.1±0.0	0.1±0.0	1.7±0.1
mNOD2	0.2±0.0	0.1±0.0	1.6±0.1

The results are provided as optical density values (650 nm).
The values represent the means and standard deviations of three screenings.
TLR/NLR ligand screening were performed by InvivoGen, as described in Methods.
doi:10.1371/journal.pone.0106807.t001

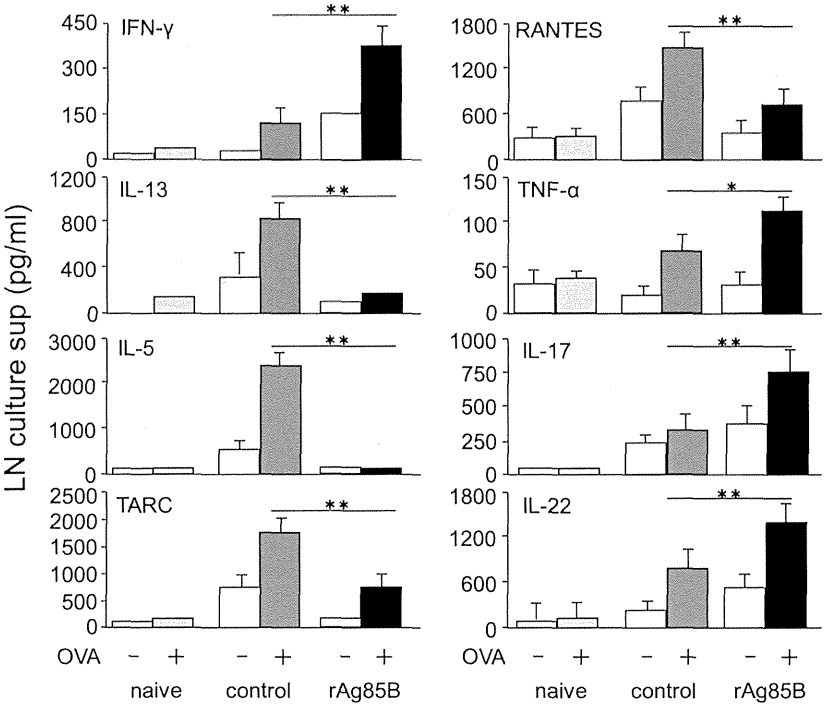

Figure 2. Administaration of rAg85B induced immune deviation from a Th2-response towards a Th1, Th17-related response in OVA-stimulated LN cells. OVA-immunized (i.p., day0 and 14) and sensitized (5% aerosolized-OVA, day21 to 25) BALB/c mice were challenged with PBS or rAg85B protein (i.p. (100 μg; days 0 and 14) and i.n. (20 μg; days 21, 23, and 25)). At 24 h after the last OVA sensitization, mediastinal lymph nodes (MLNs) from naïve or OVA sensitized BALB/c mice treated with PBS or rAg85B, were harvested. MLNs were cultured with OVA (50 μg/ml), and cytokines in the culture supernatant were determined 48 h after incubation by ELISA. Data are representative of at least three independent experiments (*P<0.05, **P<0.01 compared with OVA control. error bars, s.d.; n = 6 mice).
doi:10.1371/journal.pone.0106807.g002

which utilize a nuclear factor-kB inducible SEAP (secreted embryonic alkaline phosphatase) reporter gene as the read-out. These HEK293-derived cells are functionally expressing a given TLR or NOD gene from human or mouse. A recombinant HEK293 cell line for the reporter gene only was used as negative control. Positive control ligands are heat-killed *Listeria monocytogenes* (HKLM) for TLR2, Poly(I:C) for TLR3, Lipopolysaccharide (LPS); K12 for TLR4, Flagellin for TLR5, CL097 for TLR7, CL075 and poly(dT) for TLR8, CpG ODN for TLR9, C12-iEDAP for NOD1, and L18-MDP for NOD2. rAg85B (10 μg/mL) was added to the reaction volume. TLR/NLR ligand screening were performed by InvivoGen.

Statistical analysis

Data are shown as means±SD. Statistical significance of differences between the OVA-control group and rAg85B-treated group was assessed by the non-parametric Mann-Whitney U-test. Statistical comparisons between groups of rAg85B+isotype control and rAg85B+neutralization antibody were performed using the non-paramatric Kruskal-Wallis H-test.

Results

Effects on allergic inflammation by administration of rAg85B

To investigate the role of rAg85B in pulmonary allergic inflammation, we examined the frequently used mouse model of ovalbumin (OVA)-induced allergic lung inflammation. The mice were intraperitoneally (i.p.) (days 0 and 14) and intranasally (i.n.) (days 21, 23, and 25) administered with rAg85B (Fig. 1*A*). The purity of rAg85B was evaluated by silver staining of SDS-PAGE gel (Fig. S1) and the Limulus Amebocyte Lysate (LAL) assay (less than 0.02 EU (endotoxin units)/ml). Furthermore rAg85B was not contaminated with any TLR/NLR binding immune stimulants (Table 1). Twenty-four hours after the final OVA challenge, inflammatory cell recruitment into the lungs was analyzed. The OVA-induced allergic manifestation was suppressed with a decrease in the total number of bronchoalveolar lavage (BAL) cells and serum IgE level in the rAg85B-administered mice (Fig. 1*B*, *1C*). A marked reduction in eosinophil (Gr-1(+)/Siglec-F(+)) infiltration was observed by flow cytometric (FACS) analysis of BAL in rAg85B-administered mice (Fig. 1*D*). In association with decreased eosinophilia, neutrophil (Gr-1(+)/Siglec-F(-)) recruitment was seen in rAg85B-administered mice (Fig. 1*D*). These results were confirmed by histopathological observation of hematoxylin and eosin (H&E) staining (Fig. 1*E*). Mice administered rAg85B showed inhibition of infiltration of cells. (Fig. 1*E*). Lung sections were also stained with Masson's trichrome to evaluate fibrosis, and stained with α-smooth muscle actin. Sizes of both the peribronchial smooth muscle area and lung fibrosis area were increased in OVA-sensitized control mice; however, mice administered rAg85B showed strong suppression of both fibrosis and α-smooth muscle actin expression as well as reduction in inflammation severity assessed by H&E staining (Fig. 1*E*). These observations indicated that rAg85B has a critical function of regulating airway inflammation in a mouse model of allergen-induced asthma. Moreover, rAg85B i.n. administration induced wound repair including suppression of both fibrosis and α-smooth

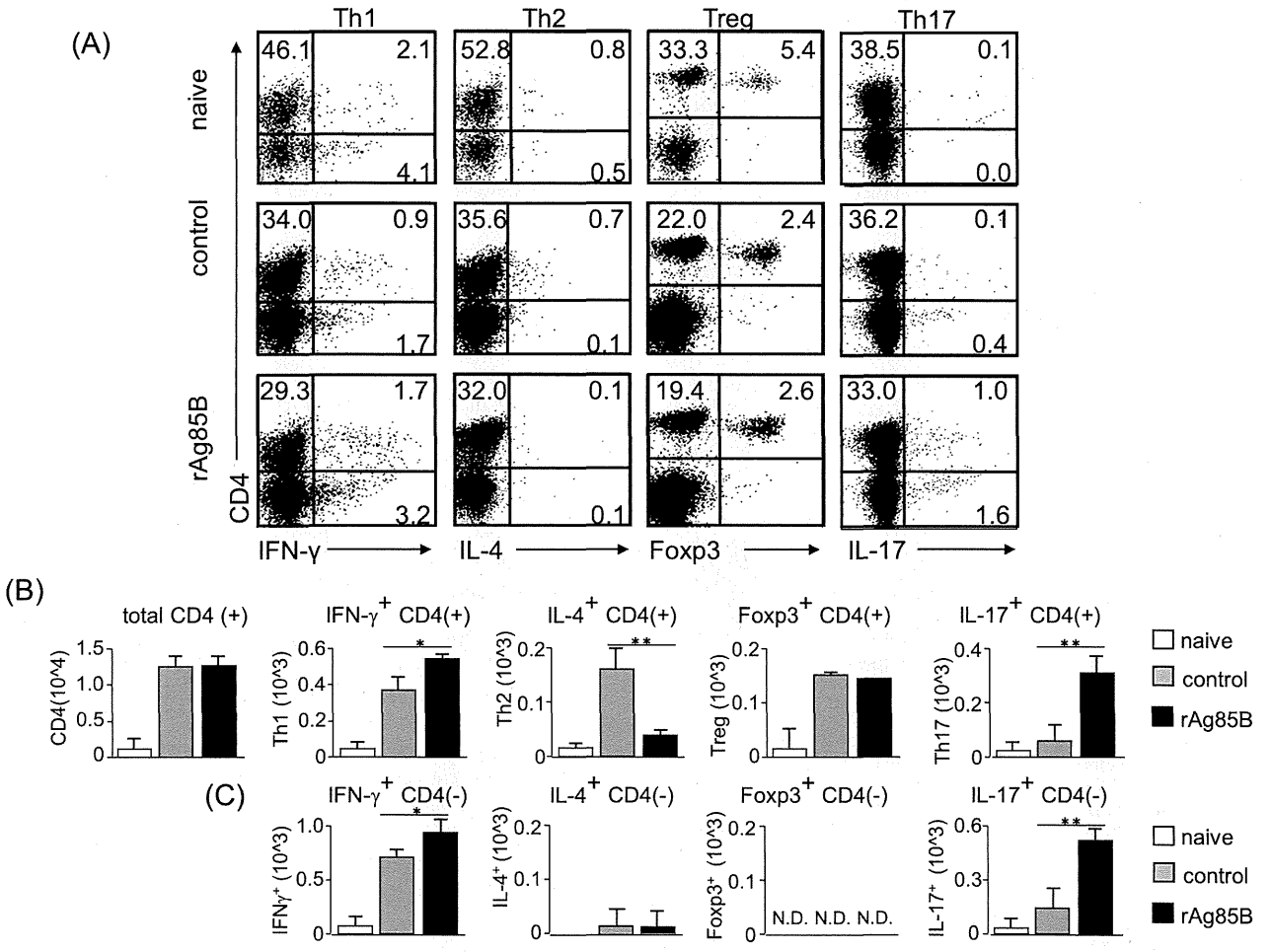

Figure 3. IFN-γ and IL-17-producing CD4 T cell subsets proliferated in lymph nodes after rAg85B administration. OVA-immunized (i.p., day0 and 14) and sensitized (5% aerosolized-OVA, day21 to 25) BALB/c mice were challenged with PBS or rAg85B protein (i.p. (100 μg; days 0 and 14) and i.n. (20 μg; days 21, 23, and 25)). At 24 h after the last OVA sensitization, mediastinal lymph nodes (MLNs) from naïve or OVA sensitized BALB/c mice treated with PBS or rAg85B, were harvested. MLNs were stimulated with ionomycin and PMA for 5 h, and with brefeldin A added in the last 3 h. Flow cytometry of stimulated MLNs from naïve (upper), PBS-treated (middle) and rAg85B protein-treated (lower) OVA-sensitized mice stained with specific antibodies indicated marker. Numbers in quadrants indicate percent of cells in each (*A*). Absolute numbers of various cell populations (above graphs) in lymph nodes (*B, C*). Data are representative of three independent experiments (*P<0.05, **P<0.01 compared with OVA control. error bars, s.d.; n = 6 mice).
doi:10.1371/journal.pone.0106807.g003

muscle actin expression. Incidentally, previous data showed that either i.p. (days 0, 14) or i.n. (days 21, 23, and 25) challenge with rAg85B did not induce strong suppression of Th2-response in OVA-sensitized mice (data not shown).

Immune deviation from a Th2-response towards a Th1, Th17-related response by rAg85B administration

We next assessed the production of OVA-specific cytokines in lymph node cells after *in vitro* stimulation with OVA (Fig. 2). Cells from mediastinal lymph nodes (mLNs) were stimulated *in vitro* with OVA and the production of various types of cytokines was assessed. The level of the Th1 cytokine IFN-γ in culture supernatants of cells from rAg85B-administered mice was increased. On the other hand, the levels of Th2 cytokines IL-5 and IL-13 in culture supernatants of cells from rAg85B-administered mice were lower than those in culture supernatants of cells from control mice. Similarly, mice administered rAg85B showed inhibition of production of the CCL5 (RANTES) and the thymus- and activation-regulated chemokine CCL17 (TARC), which contribute to allergic inflammation. Production of IL-17, IL-22 and TNF-α was also enhanced in culture supernatants of OVA-stimulated mLN cells from rAg85B-administered mice. These results suggested that Th1 and Th17 cytokines are crucial factors in the suppressive effect of rAg85B on airway inflammation.

$CD4^+$ T cells producing IFN-γ and IL-17 were increased in mediastinal lymph nodes by rAg85B administration

We next examined Th cell responses in the mouse asthma model by intracellular staining analysis. mLN cells were stimulated with or without PMA and ionomycin, and cell fractions were analyzed by intracellular cytokine staining. Stained $CD4^+$ T cells producing IFN-γ or IL-17 were increased in mice administered rAg85B, whereas IL-4-secreting cells were decreased in those mice (Fig. 3*A*, *3B*). On the other hand, rAg85B administration was not associated with the induction of Treg cells, which express Foxp3

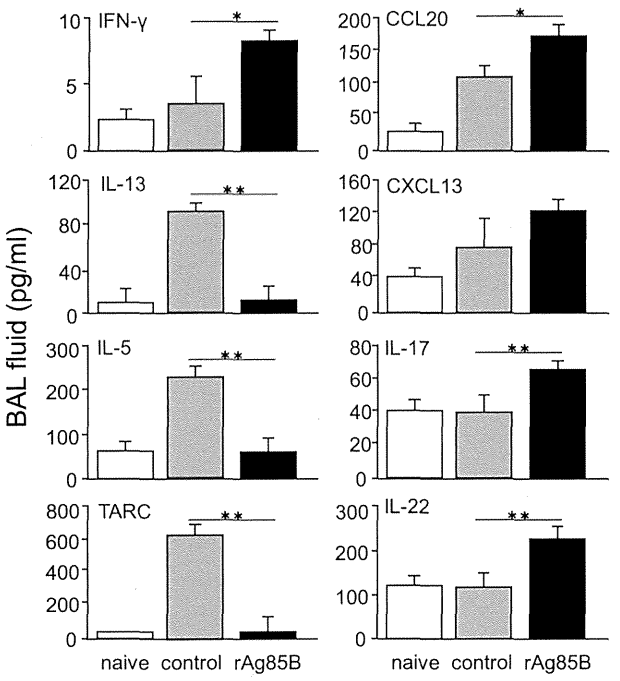

Figure 4. Administration of rAg85B resulted in the reduction of Th2 cytokine and chemokine levels and in the enhancement of Th1 and Th17 cytokine levels in BAL fluid. OVA-immunized (i.p., day0 and 14) and sensitized (5% aerosolized-OVA, day21 to 25) BALB/c mice were challenged with PBS or rAg85B protein (i.p. (100 μg; days 0 and 14) and i.n. (20 μg; days 21, 23, and 25)). At 24 h after the last OVA sensitization, BAL fluid from naïve or OVA sensitized BALB/c mice treated with PBS or rAg85B, were harvested. Levels of cytokines in the BAL fluid were measured directly by ELISA. Data are representative of at least three independent experiments (*P<0.05, **P<0.01 compared with OVA control. error bars, s.d.; n = 6 mice).
doi:10.1371/journal.pone.0106807.g004

and CD25, in LNs (Fig. 3*A*, *3B*, S2). These results were the same for not only the fraction of $CD4^+$ T cells but also the fraction of $CD4^-$ cells producing cytokines in mLNs (Fig. 3*C*). These results suggested that rAg85B administration was involved in the induction of IFN-γ or IL-17-producing $CD4^+$ T cells and $CD4^-$ cells in LNs.

Mice administered rAg85B showed reduction in levels of Th2 cytokines and chemokines levels and increase in levels of Th1 and Th17 cytokines in BAL

The pathogenesis of asthma is associated with many cell types and several molecular/cellular pathways in the lung. Therefore, we investigated whether rAg85B administration regulates various cytokines associated with the pathogenesis of allergic inflammation in BAL fluid. Control mice in which allergic inflammation developed showed increased production of Th2 cytokines and chemokines in BAL fluid, such as IL-13, IL-5 and TARC. Mice administered rAg85B showed inhibition of the induction of IL-13, IL-5 and TARC (Fig. 4). Furthermore, enhancement of IFN-γ, IL-17 and IL-22 production was observed in BAL fluid from mice administered rAg85B. Production of chemokines secreted from non-T cells, CCL20 and CXCL13, was also increased in BAL fluid from rAg85B-administered mice. The chemokine CCL20 is thought to be associated with the recruitment of Th17 lymphocytes and LTi-like or NK-like cells [17,18], and CXCL13 is a chemokine ligand of C-X-C motif receptor 5 (CXCR5) that is expressed on Lti-like cells. These findings suggested that rAg85B administration was involved in induction of immune responses from both $CD4^+$ T cells and other innate cells in BAL fluid of mice in which allergic inflammation has developed.

rAg85B administration elicits IL-17-producing CD4-negative cells rather than $CD4^+$ T cell subsets in BAL fluid

To determine the peripheral Th cell population in the lungs of rAg85B-treated mice, BAL cells from experimental mice were analyzed by intracellular cytokine staining. The percentages of IFN-γ and IL-17-positive cells from rAg85B-administered mice were higher than those from control cells in agreement with the results of FACS analysis of mLN cells (Fig. 5*A*), and Treg cells in BAL fluid from rAg85B-administered mice were also the same as the results for mLN cells (Fig. 5*A*). The absolute number of $CD4^+$ T cells stained for IL-17 was not increased in BAL cells from rAg85B-administered mice, unlike the results for mLN cells; however, total IL-17-secreting cells, $CD4^-$ $IL\text{-}17^+$ cells, were increased in rAg85B-administered mice compared with those in control mice (Fig. 5*B*, *5C*). $CD4^-$ IFN-γ-producing cells were observed in BAL fluid from rAg85B-administered mice as same to $CD4^+$ cells. In addition, IL-4-secreting $CD4^+$ cells were decreased in rAg85B-treated mice, whereas IL-4-producing $CD4^-$ cells were not observed. These observations indicated that IL-17 was produced by $CD4^-$ cells rather than by $CD4^+$ T cells in BAL, unlike IFN-γ and IL-4. Furthermore, the types of BAL cells greatly changed after rAg85B treatment (Figure S3).

rAg85B administration was involved in recruitment of innate immune cells that secrete IL-17-related cytokines in BAL fluid

Recent studies have demonstrated that IL-17 was not only secreted by Th17 cells and the source of Th17-related cytokines was modified in various environmental conditions [19]. Mice administered rAg85B showed infiltration of CD4-negative immune cells, which secreted IL-17 cytokine in BAL fluid (Fig. 4, Fig. 5). From these findings, we next investigated the proportions of infiltrating $CD4^-$ cells that produce IL-17, including γδT cells, $IL\text{-}7R^+$ Lin^- cells (LTi-like cells), $CD3^-$ $NKp46^+$ cells and $CD11c^+$ cells, in BAL fluid from experimental mice. OVA-sensitized BALB/c mice administered rAg85B, but not mice administered PBS, showed an increased number of innate immune cells in BAL fluid (Fig. 6*A*). The percentages of $CD4^+$ and $CD8^+$ T cells in BAL fluid from rAg85B-administered mice were similar to those in BAL fluid from control mice. However, the percentages of γδT cells, LTi-like cells, $NKp46^+$ cells, and $CD11c^+$ cells in BAL fluid from rAg85B-administered mice were higher than those in BAL fluid from control mice (Fig. 6*A*). Since innate immune cells, which secrete IL-17 and related cytokines, IL-22, were thought to be induced by rAg85B administration, we next explored the source of IL-17-related cytokines in BAL fluid. Small numbers of IL-17-producing γδT cells, LTi-like cells and $CD11c^+$ cells were observed (Fig. 6*D*, *6F*, *6G*), while production of IL-17 from CD8+ T cells and $NKp46^+$ cells was not detected (Fig. 6*C*, *6E*). In the present study, a Th17-related cytokine, IL-22, was also detected in BAL fluid from mice administered rAg85B. (Fig. 4). All of the cells from BAL secreting Th17-related cytokines, including $CD4^+$ T cells, γδT cells, $NKp46^+$ cells, LTi-like cells and $CD11c^+$ cells, that were examined in this study showed IL-22 production in mice administered rAg85B (Fig. 6*B*, *6D*, *6E*, *6F*, *6G*). On the other hand, production of IL-17 from $NKp46^+$ cells and $CD11c^+$ cells were not detected (Fig. 6*E*, *6G*). Although it is now known that NKT cells, alveolar macrophages and neutrophils might also